Journal of Chromatography, 159 (1978) 147–181
Chromatographic Reviews

CHREV. 110T11

SOME CURRENT AND POTENTIAL USES OF MAGNETIC FIELDS IN ELECTROKINETIC SEPARATIONS

ALEXANDER KOLIN
Institute of Molecular Biology, University of California, Los Angeles, Calif. (U.S.A.)

CONTENTS

1. IDEAS WHICH LED TO USES OF MAGNETIC FIELDS IN ELECTROKINETIC SEPARATIONS

I always find it instructive to attempt to reconstruct the sequence of ideas which lead to a given scientific development. In retrospect it seems to me that there is a thread of continuity which leads from my work on electrophoresis and electromagnetophoresis back to a seemingly completely unrelated development, namely, the electromagnetic method for measuring blood flow.

In 1935[1,2] I set myself the goal of developing a method for measuring the flow of blood in an artery without opening or penetrating its wall. The idea which led to the solution came to me as an analogy to the Hall effect. If we send a current (represented by vector $\vec{V} = \vec{J}$ in Fig. 1) through a cylindrical conductor, such as a wire (C in Fig. 1), while maintaining a magnetic field ($\vec{B}$) at right angles to the current, an e.m.f. (the Hall voltage) can be detected by the meter MS across a cylinder diameter (between the electrodes E_1 and E_2) perpendicular to the magnetic field. If we imagine

positive as well as negative charge carriers to be present in the conductor they will be moved in opposite directions along the x-axis direction by the current source. The Lorentz force exerted upon these moving charges at right angles to the magnetic field will, however, be in the same direction for the positive as well as negative charges because their signs as well as directions of motion are mutually opposite. Thus, if the charge densities of both charge carriers were the same, there would be no potential difference across a cylinder diameter in the direction of the Lorentz force (z-axis) since opposite charges are moved in the same direction. The Hall effect is of great importance to determine the sign and space-density of electrons or holes in semiconductors from the sign and magnitude of the Hall coefficient $R = 1/nec$, where n is the space density of the electrons, e the electron charge and c the velocity of light. In electrolytes, however, freely moving ions of opposite sign are present in equal concentration and the Hall voltage detected between electrodes E_1 and E_2 is zero.

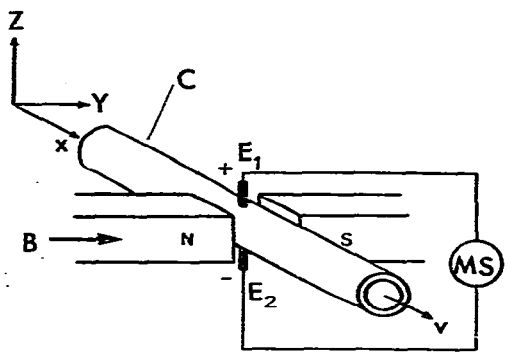

Fig. 1. Cylinder C between magnet poles N and S. $\vec{B}$, magnetic field vector; E_1 and E_2, electrodes; $\vec{V}$, vector specified in text; MS, instrument specified in text.

It occurred to me that this latter situation will be drastically changed if, instead of moving the charge carriers in opposite directions by an electric field, we would move them in the same direction by fluid flow through a pipe C in Fig. 1 across a magnetic field. In this case the Lorentz forces will act in opposite directions on the charge carriers of opposite sign and we will obtain a charge separation and an electric field opposing the Lorentz force. The charge separation will proceed until the electric field produced by it balances the Lorentz field $\vec{E}$ seen by the charges moving with velocity $\vec{v}$ across the magnetic field $\vec{B}$ ($\vec{E} = [\vec{v} \times \vec{B}]$). Our meter MS will then detect a potential difference between the electrodes E_1 and E_2 contacting the fluid which will be proportional to the fluid velocity $\vec{v}$ and we would have an electromagnetic flow meter before us. Material properties like electrical conductivity or space density of charge carriers do not appear in our equations so that the reading of the meter MS will be the same for all fluid conductors in a given field $\vec{B}$ at a given fluid velocity $\vec{v}$. What we have just described is nothing other than the process of electromagnetic induction in a moving fluid. It is in terms of this more familiar concept that this idea has been described in the literature[1,2].

After demonstrating the above effect in electrolytes and using it to measure blood flow with electrodes making contact with the outside of an artery wall, it occurred to me that this effect could be inverted. By replacing the meter MS with a current source and sending an electric current through the electrolyte between the electrodes E_1 and E_2 in the transverse magnetic field $\vec{B}$, a force was exerted upon the electrolyte in the direction of the x-axis and the fluid was set in motion in the direction of the vector $\vec{V}$ in Fig. 1. The rate of pumping was so embarrassingly small and the experiment looked so obvious that I did not take the trouble to publish it. This magnetohydrodynamic pumping action has, however, found in recent times many important uses and I have utilized it in an electrophoretic application that will be described in the last section of this paper.

2. ELECTROMAGNETOPHORESIS

The above experience undoubtedly triggered the following question which occurred to me in the midst of a lecture to medical students. I was describing how the Lorentz force exerted upon ions in an electrolyte-filled rubber tube carrying a current across a magnetic field is transmitted by the ions to the tube. I suddenly visualized a sphere suspended in the tube and asked myself if an object surrounded by the current-carrying electrolyte under these conditions would experience a force like the tube wall. A little thought after the lecture led me to the conclusion that a dielectric sphere would indeed experience a force but that the force would be opposite to the force exerted upon the wall of the rubber tube. It soon became clear that the force would be zero upon a suspended object of an electrical conductivity matching that of the surrounding electrolyte. It would have the same direction as the force upon a tube for a body of higher electric conductivity than the electrolyte and would point in opposite direction for a body of lesser conductivity than the electrolyte. It soon became clear that this was a phenomenon having more resemblance to gravitational sedimentation than to electrophoresis and that its dependence on the relative conductivities of the suspended object and the ambient electrolyte was analogous to the phenomena of flotation governed by Archimedes' principle. I called this effect electromagnetophoresis[3,4]. Even an approximate theory of this phenomenon is rather complex[5,6]. We shall consider it here in a simplified rough approximation.

Fig. 2 shows an apparatus in which this effect can be observed. A Helmholtz coil pair generates a magnetic field $\vec{B}$. A migration cell placed between the coils has the shape of a parallelepiped whose top and bottom surfaces are metallic and serve as electrodes E_1 and E_2, while the remaining walls are made of dielectric material. The current density $\vec{J}$ maintained through the electrolyte between the electrodes is perpendicular to the magnetic field $\vec{B}$. The force density, *i.e.* the force per unit volume exerted upon the electrolyte is

$$\vec{F}^* = [\vec{J} \times \vec{B}] \tag{1}$$

(where $\vec{F}^*$ is in dynes/cm^3, $\vec{J}$ in abamperes/cm^2 and $\vec{B}$ in gauss). This force is analogous to the weight density, the force exerted upon a unit volume in the gravitational field.

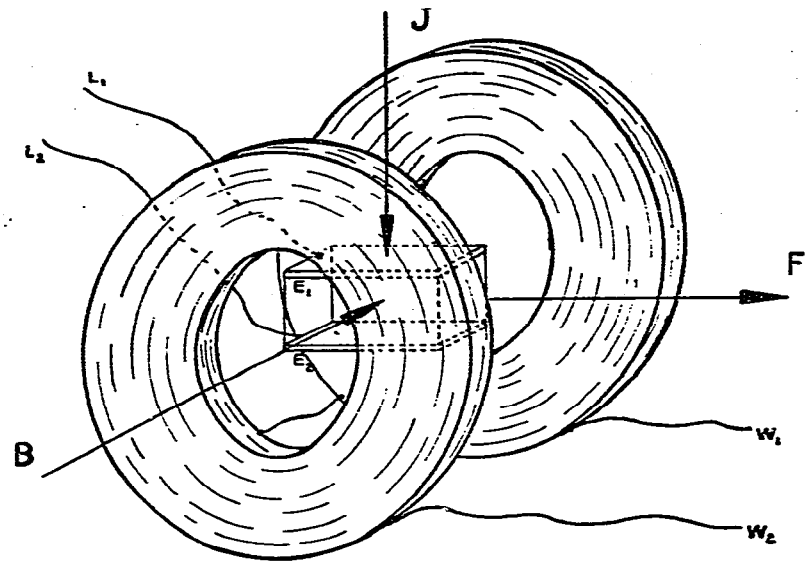

Fig. 2. Arrangement for demonstration of electromagnetophoresis. A migration cell with electrodes E_1 and E_2 is placed between two Helmholtz coils. $\vec{B}$, magnetic field vector; $\vec{J}$, current density vector; $\vec{F}$, electromagnetic force; w_1, w_2, coil lead wires; L_1, L_2, electrode leads. (From A. Kolin, *Proc. Ist Nat. Biophys. Conf.*, Yale University Press, 1959.)

We shall consider the horizontal electromagnetic force field as a quasi-gravitational field. While the gravitational force generates a pressure gradient in the fluid so that the pressure increases in the downward direction, the horizontal quasi-gravitational force in Fig. 2 similarly generates a horizontal pressure gradient with the hydrostatic pressure increasing in the direction of the $\vec{F}$ vector. For simplicity, we shall imagine that our experiment is performed in a freely falling system, such as a satellite in orbit where there are no gravitational manifestations, so that the electromagnetic force field is the only field to be considered.

As a consequence of the downward increase in pressure in a gravitationally induced fluid pressure gradient, the hydrostatic pressure is highest at the lowest points of a submerged object and lowest at the highest points. If we calculate the resultant pressure force exerted upon the surface of the submerged object by integration over its entire surface, we obtain a force pointing in the direction of diminishing pressure (*i.e.* opposite to the force of gravity) of a magnitude equal to the weight of the ambient fluid displaced by the submerged body. This is, of course, the well known force of buoyancy. Similarly, we can perform an analogous calculation in our electromagnetic force field generated as shown in Fig. 2. The result is a surface force $\vec{F}_s$ experienced by each volume element of the electrolyte as a result of the ambient fluid pressure gradient. The direction of this force is, as in the gravitational case, opposite to the force $\vec{F}$ of Fig. 2. In fact, this force is analogous to the force of buoyancy in the gravitational field. It will be convenient for us to adopt a similar terminology, referring to this surface force as "electromagnetic buoyancy" and to the opposite force exerted upon the interior of the volume element as "electromagnetic gravity".

We can now understand why a non-conducting submerged object like a

dielectric sphere will experience a force in the electrolyte-filled cell of Fig. 2 in spite of the fact that it passes no current, so that no electromagnetic forces can be exerted upon its interior. What it suffers is the surface force of electromagnetic buoyancy which is opposite to the direction of the force which generates the pressure gradient in the ambient fluid. If the submerged object is a conductor, it passes a current and its interior experiences a force, "electromagnetic gravity" (EMG) (in the direction of force $\vec{F}$ of Fig. 2), in addition to the opposite surface force of "electromagnetic buoyancy" (EMB). The net force upon the body is the sum of EMB and EMG. In the case of an object whose electrical conductivity σ' is identical with the conductivity σ'' of the surrounding fluid the forces of EMG and EMB are equal and opposite and the resultant force is zero in analogy to isopyknic equilibrium in the gravitational field.

The quantity which is analogous to the density in our gravitational analogy is the electrical conductivity σ. Fig. 3 shows how the value σ' of the conductivity of a body submerged in a fluid of conductivity σ'' affects the current density in the body. The sphere of $\sigma' = \sigma''$ in Fig. 3A is "electrically transparent". The current traverses it without change in current density. Since the current density $\vec{j}$ in the body interior determines the value of the volume force density $\vec{F} = [\vec{j} \times \vec{B}]$, we see that EMG + EMB = 0 in this case and we will not expect a particle of this electrical conductivity to migrate in the given electrolyte.

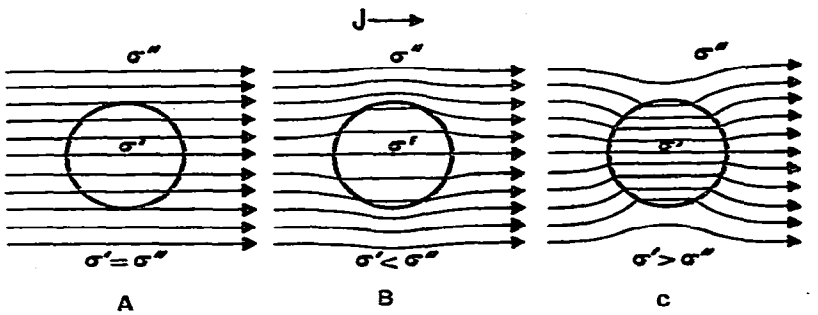

Fig. 3. Refraction of electric current lines. Distribution of current density in a sphere of conductivity σ' in a surrounding fluid of conductivity σ''. (A) $\sigma' = \sigma''$; (B) $\sigma' < \sigma''$; (C) $\sigma' > \sigma''$. In all cases the current density inside the sphere is uniform. It is the same as in the surrounding fluid in A, diminished in B, and increased in C. [From A. Klin, *Science*, 117 (1953) 134.]

On the other hand, we see in Figs. 3B and 3C how the current distribution is changed by suspended spheres when $\sigma' \neq \sigma''$. Such changes in current distribution with concomitant refraction of the electrical current lines at the interface have been calculated by Maxwell[7]. We see in Fig. 3B how the current tends to flow around a poor conductor ($\sigma' < \sigma''$) in which the current density is less than at "infinite" distance in the ambient fluid. Consequently EMG < EMB in this case. The surface force predominates over the volume force and the sphere moves opposite to the direction of the $\vec{F}$ vector in Fig. 2. On the other hand, the superior conductor ($\sigma' > \sigma''$) tends to concentrate the current lines in its interior, thus increasing the current

density in it above the value of $\vec{J}$ in regions of unperturbed current density. Such a more highly conductive object will act similarly to a denser body suspended in a fluid in the field of gravity. It will move in the direction of the force exerted upon the fluid volume as a whole (direction of $\vec{F}$ in Fig. 2). Thus two species of particles of conductivities σ_a' below and σ_b' above the conductivity σ'' of the ambient fluid would move in opposite directions and be easily separated.

Calculations[3-5] valid for particles of cellular dimensions (radius $a \lesssim 10^{-2}$ cm) yield the following equations from which the forces (F) upon and migration velocities (v) of spherical particles of radius a and of conductivity σ' suspended in a fluid of conductivity σ'' and viscosity η can be calculated:

$$F = 2\pi a^3 [J \times B] \left(\frac{\sigma' - \sigma''}{\sigma' + 2\sigma''}\right) \tag{2}$$

$$v = JB \left(\frac{\sigma' - \sigma''}{\sigma' + 2\sigma''}\right) \frac{a^2}{3\eta} \tag{3}$$

We see from both equations that the force and velocity vanish for $\sigma' = \sigma''$ and that their signs reverse as the value of σ' increases from $\sigma' < \sigma''$ to $\sigma' > \sigma''$.

A numerical example will give an idea of the order of magnitude of this effect. We assume non-conducting particles ($\sigma' = 0$) of radius $a = 10^2\,\mu\text{m} = 10^{-2}$ cm, $J = 0.1\ A/\text{cm}^2$, $B = 10^4$ gauss, $\eta = 10^{-2}$ poise. Eqn. 3 yields for this case $v \approx 1.67$ cm/sec or 83.5 diameters/sec. Superconducting magnets of much higher intensity than assumed here are currently available permitting to obtain much greater migration speeds at higher magnetic fields.

In addition to the capability of electromagnetophoresis to discriminate between particles of different radius (a) and electrical conductivity (σ') as suggested by eqn. 3, it offers the possibility to separate particles on the basis of differences in shape as suggested by Fig. 4 (refs. 3, 4). We shall consider the sphere of Fig. 3C ($\sigma' > \sigma''$) and imagine it deformed (without change in volume) into a prolate spheroid seen in Fig. 4A. The concentration of the current in the submerged body is much greater for

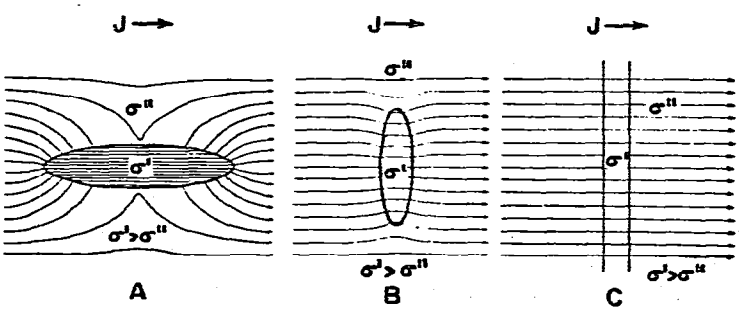

Fig. 4. Effect of shape on current density j inside a body of conductivity σ' immersed in a fluid of conductivity $\sigma'' < \sigma'$. (A) Prolate spheroid: current lines are strongly refracted at interface and internal current density is uniform and greatly increased as compared to unperturbed current field. (B) Oblate spheroid: internal current density is only slightly increased. (C) Infinitely wide disk (lateral view): no refraction of current lines; internal and external current densities are equal. [From A. Kolin, *Science*, 117 (1953) 134.]

this shape and orientation than for a sphere of equal conductivity[3,4] as depicted in Fig. 4A. In view of the greatly increased internal current density j', the submerged body will act like a body of greatly increased electromagnetic weight density. Thus, suspended particles differing but little in electrical conductivity and volume could be separated on the basis of differences in shape which would produce a difference in electromagnetic weight densities.

A deformation of our sphere into an oblate spheroid as shown in Fig. 4B would have a different effect. The internal current density j' in this body will be less than for a sphere of equal volume and conductivity σ'. The oblate spheroid will thus behave like a body of lesser electromagnetic weight density than the sphere of equal volume and conductivity and will exhibit a much smaller electromagnetic weight-density than an equiconductive prolate spheroid of equal volume[3,4]. The plate of conductivity σ' can be considered as a limiting case of a prolate spheroid whose thickness is vanishingly small as compared to its lateral dimensions. There is no refraction of current lines in this case depicted in Fig. 4C for the shown orientation. The current density in the plate is the same as outside. The forces of EMB and EMG thus cancel each other and the conductive plate placed perpendicular to the current experiences no force.

Table I illustrates effects of orientation of a cylinder upon the current density in it, and thus upon the manifested electromagnetic weight density[4,5].

TABLE I

ORIENTATION-DEPENDENCE OF FORCE UPON A CYLINDER

Body	*Orientation**	*Force density F*	*Special conditions*
Sphere		$\frac{3}{2}[JB]\left(\frac{\sigma'' - \sigma'}{2\sigma'' + \sigma'}\right)$	
Cylinder	$\vec{B}$	0	
Cylinder	$\vec{J}$	$[JB]\left(\frac{\sigma'' - \sigma'}{\sigma''}\right)$	$\frac{L}{a} \gg \frac{\sigma'}{\sigma''}$
Cylinder	$\vec{F}$	$[JB]\left(\frac{\sigma'' - \sigma'}{\sigma'' + \sigma'}\right)$	

* Cylinder axis parallel to vector indicated.

We have treated electromagnetophoresis so far, as if it were produced by a combination of a constant magnetic field with a perpendicular direct current. Actually, this is not necessarily the most favorable case because of electrolysis at the electrodes. By periodically reversing the magnetic field in phase with reversals of the electric current we exert a unidirectional force upon suspended particles. The use of an alternating current has another aspect of interest. A biological cell is not an homogeneous conductor. The cell interior is surrounded by a cell membrane which can be, electrically, roughly approximated by an equivalent circuit of a resistance in series with a parallel combination of resistance and capacitance. The impedance of the

cell membrane is thus frequency-dependent and so will be the density of the electric current passing through the cell. We thus gain a further parameter, the frequency characteristics of the cell membrane impedance, according to which biological cells may be separated by electromagnetophoresis.

In our gravitational analogy we consider electromagnetophoretic migration as an analog to gravitational sedimentation. The analogy can also be extended to centrifugation. We can produce a radial electromagnetic force field in which particles differing from the suspension fluid in the value of the conductivity σ will migrate either toward a center of convergence or away from it, just as they would in a centrifuge on the basis of density differences[8].

Fig. 5 shows the simplest kind of electromagnet, a wire W carrying an electric current which generates a solenoidal magnetic field (H). (Actually a water-cooled copper tube passing an a.c. current of 3,500 A derived from a step-down transformer was used). The wire passes through a cylindrical migration cell whose flat walls serve as electrodes, E_1 and E_2. The current density $\vec{J}$ between the electrodes is parallel to and in phase with the current $\vec{I}$ that is passed by the wire. The circular magnetic field lines are thus perpendicular to $\vec{J}$ and the Lorentz force $\vec{F}$, being perpendicular to $\vec{J}$ and $\vec{H}$, is radial. Particles suspended in a fluid of conductivity σ'' will thus exhibit centrifugal or centripetal migration depending on the sign of $\sigma' - \sigma''$. To obtain centrifugation without rotational motion one need not use a circular cell as shown in Fig. 5. Its cross-section may be a semicircle or a sector of less than 180° angular opening could be used so that the wire W would not have to pass through the cell interior.

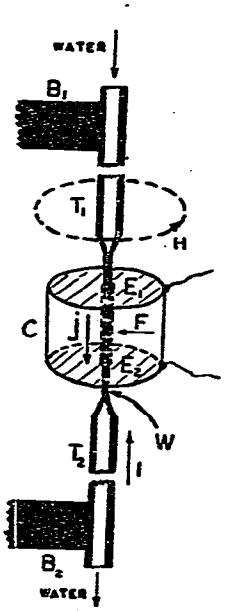

Fig. 5. Electromagnetophoretic non-rotational centrifuge. W, Conductor generating a solenoidal magnetic field; C, migration cell; E_1 and E_2, electrodes; J, current density in cell C; I, current in conductor W; T_1 and T_2, wide copper tubes linked to hollow conductor W; B_1 and B_2, current leads. [From A. Kolin, *J. Appl. Physics*, 25 (1954) 1065.]

3. ELECTROMAGNETOPHORESIS AND CURRENT INTEREST IN CELL SEPARATION METHODOLOGY

While reasonably satisfactory electrophoretic methods are currently available for cell electrophoresis[9–12], there are some serious limitations which may require development of new separation methods. To maintain a high electric field intensity and electrophoretic mobility of cells it is necessary to use buffers of low ionic strength and electric conductivity. Non-electrolytes such as sucrose must be added to avoid osmotic damage to the cells. The cells must remain for an appreciable period of time in a less than optimal environment differing considerably from their natural habitat. An ideal separation method would be one permitting, for instance, mammalian cells to remain in an environment like blood serum during the separation process.

Another drawback of electrophoresis as a method of cell separation is the usually relatively small percent difference in electrophoretic mobilities between the cell species which one is interested in separating. A separation method based on a physical parameter that varies more widely from one cell species to another would, of course, be preferable.

It appears that electromagnetophoresis holds out the promise of fulfilling the above desiderata. Unlike electrophoresis, electromagnetophoresis is carried out most effectively in a high-conductivity fluid. Blood serum would be an ideal suspension medium for cell-electromagnetophoresis. This would greatly reduce the problem of power dissipation in the cell suspension by the current. Physiological saline would also be a suitable suspension medium and the use of materials such as sucrose for achievement of osmotic balance would be unnecessary.

Of even greater importance is the fact that biological cells may differ by several orders of magnitude in values of their electric conductivities[13]. Electromagnetophoresis may thus provide a tool of exceptionally high resolution for cell separations. An added factor of interest is that the entry of the current into a biological cell will be determined by the permeability of the cell membrane to ions. There may thus be a prospect of cell separation on the basis of differences in ionic cell membrane permeabilities.

Another prospective advantage is the possibility of using alternating currents which eliminates electrolysis and greatly simplifies the design of the separation cell.

It may also be of interest to compare the electrophoretic velocities in contemporary "free-flow" electrophoresis apparatus with migration speeds achievable by electromagnetophoresis. A human erythrocyte of 25 TU electrophoretic mobility [1 Tiselius Unit (TU) $= 10^{-5}$ cm sec^{-1}/V cm^{-1} (ref. 14)] will move in the field of 100 V/cm in a free-flow or endless belt electrophoresis apparatus with a speed of 0.025 cm/sec. This speed is to be compared with electromagnetophoretic (EMP) speeds calculated from eqn. 3 for a normal laboratory electromagnet of 25 kilogauss and a superconducting magnet of 100 kilogauss. We choose round figures for radii of two types of cells: $a_1 = 5$ μm and $a_2 = 10$ μm which are in the order of magnitude of erythrocyte and lymphocyte dimensions, respectively. The calculated velocity values v are displayed in Table II. We see that the EMP-speed of the smaller cell is a little less than half of the above mentioned electrophoretic speed of an erythrocyte at the weaker magnetic field. However, the speed of the larger cell (large lymphocyte) is four times as great and much greater than the electrophoretic erythrocyte velocity.

The velocity difference between the two types of cells is large as compared to velocity differences normally encountered between such cells in electrophoresis. At the larger magnetic field intensity (100 kilogauss) both types of cells by far surpass the cited electrophoretic migration velocity of the erythrocyte. In fact, the larger cell migrates more than six times as fast and the velocity difference between the two cell types at 100 kilogauss is 300% larger than the slower cell velocity. In addition to the anticipated resolving power on the basis of cell size differences we can expect appreciable resolution on the basis of differences in electrical cell conductivities and ionic permeabilities of cell membranes.

TABLE II

MIGRATION SPEED v OF SPHERE OF RADIUS a IN MAGNETIC FIELD B AT CURRENT DENSITY J

a (μm)	B (kilogauss)	J (abamperes/cm^2)	σ' (Ω^{-1} cm^{-1})	η (poise)	v (mm/sec)
5	25	0.1	0	0.01	0.1
10	25	0.1	0	0.01	0.4
5	100	0.1	0	0.01	0.4
10	100	0.1	0	0.01	1.6

There have been very few attempts as yet to use this effect for practical separations[15,16]. Murphy *et al.*[15] described separation of erythrocytes from blood plasma and Kovalczik[16] presented an extensive theoretical analysis and experimental accounts of electromagnetophoresis in porous media. There are probably several reasons for the long delay in utilization of this effect. (1) Electromagnetic convection due to non-uniformity of the magnetic field and of the electrical current density along with thermal convection present formidable experimental difficulties the solution of which will require no less ingenuity than went into the development of electrophoretic methods by Tiselius and those who followed him. (2) Powerful electromagnets, especially superconducting magnets, in the order of 100 kilogauss became commercially available relatively recently and are still rather costly to acquire and to operate. (3) The interest in cell electrophoresis is also of relatively recent date and it is mainly in connection with cell separations that EMP could find applications with present technology.

4. ISOPERICHORIC FOCUSSING EFFECTS: ISOCONDUCTIVITY AND ISOMAGNETIC FOCUSSING; DIGRESSION TO ISOELECTRIC FOCUSSING

In above descriptions we took it for granted that the electrical conductivity of the electrolyte was uniform throughout the EMP cell. This need not be so. We can extend our gravitational analogy by remembering the method of determination of the specific gravity of small and irregularly shaped objects. We generate a density gradient column such that the object finds a level of density equal to its own someplace within the fluid column. The determination of the fluid density at the level where the object resides yields then its density. We could now similarly create a gradient of electrical conductivity in, say, a vertical column in which we could establish a vertical EMP force. If the conductivity σ'' increases in the downward

direction we have an analogy to a stable density gradient column. Suppose the EMP column contains a suspension of cells of electrical conductivity σ'. At a certain level L_0 of the conductivity gradient column the value of the ambient conductivity will be equal to the cell conductivity: $\sigma_0'' = \sigma'$. The EMP force will not affect the cells at this level. Below this level $\sigma' < \sigma''$ and the EMP buoyancy predominates over the EMP gravity moving the cells upward toward the L_0 level. Conversely $\sigma' > \sigma''$ above the L_0 level and the cells are moved downward toward the level where $\sigma' = \sigma''$. Eventually all of the suspended cells will be swept from above and below toward the L_0 level where they will be focused in an equiconductive zone of the column.

This consideration could have led me to the idea of isoelectric focussing, but actually it did not since I was not thinking about electrophoresis at the time I worked on EMP. It was the above mentioned experimental convection difficulties[17,18] which induced me to switch temporarily to the study of electrophoresis in order to seek ideas that could be usefully transferred to electromagnetophoresis. The idea of isoelectric focussing occurred then in the process of reading about the pH dependence of the charge and electrophoretic mobilities of proteins[19–21].

Further thought about the isopyknic, isoconductivity and isoelectric focussing effects led to the insight that they are special cases of a class of effects which one might call isoperichoric focussing effects (from the Greek word "perichoron" = environment)[21]. These effects occur in a gradient of an environmental parameter (*e.g.* density) where forces are exerted upon suspended particles in those regions of the gradient column where the environmental parameter and the corresponding particle parameter differ. These forces vanish in the "isoperichoric zone" where the force-determining particle parameter equals the corresponding environmental parameter. On either side of this equilibrium zone the forces exerted upon the particles point toward this zone of convergence. By inverting the gradient one can reverse these forces so that the particles would tend to flee the isoperichoric zones (but this condition is in most cases unstable).

A predicted isoperichoric effect which may find applications in cell separations is isomagnetic focussing[21]. There are two possibilities: isodiamagnetic and isoparamagnetic focussing. We will briefly qualitatively outline isoparamagnetic focussing. A paramagnetic body in a non-homogeneous magnetic field will experience a force in the direction of increasing field intensity. Faraday discovered, however, that this was only true if the paramagnetic body was in an environment of smaller magnetic permeability. If the magnetic permeability μ'' of the environment surpasses that of the body (μ'), the latter will experience a force away from the region of maximum field strength. Let us imagine now a vertical column filled with a paramagnetic liquid whose magnetic permeability increases in the downward direction. Let us also assume that this fluid column is in a non-homogeneous magnetic field which increases in the downward direction. Each fluid element will thus experience a downward force and a pressure gradient will be established in the liquid column. The force per unit volume will be greater in proportion to the magnetic permeability of the volume element. In view of the existence of grad μ'' with a μ'' value increasing in the downward direction, we have a situation analogous to a stable density gradient in a gravitational field.

A particle of permeability μ' suspended in this permeability gradient column in a non-uniform magnetic field will experience a downward or an upward force

depending on whether it finds itself above or below the isoparamagnetic zone Z_0 where $\mu' = \mu_0''$. As in the analogy of isopyknic focussing in a density gradient, the paramagnetic particles will be eventually swept into the isomagnetic zone Z_0. Particles of a different permeability μ^* will be focussed in a different isomagnetic zone. Analogous focussing could be obtained with diamagnetic particles suspended in a diamagnetic fluid.

5. CONDUCTIVITY-GRADIENT STABILIZATION AGAINST THERMAL CONVECTION

Density gradients proved very useful for establishing concomitant pH gradients[19] and stabilization in isoelectric focussing as well as for generation of electrophoretic mobility spectra[22,23] and found uses in non-electrokinetic separation procedures. A possibility of establishing stabilizing gradients by other means and, especially, of reinforcing the stabilizing action of density gradients by other types of gradients are therefore of interest. It turns out that one can actually produce very steep stabilizing gradients in conductivity gradient columns and add their stabilizing action to that of a density gradient, thus enhancing the latter's effectiveness in suppressing thermal convection[24].

Fig. 6 shows a cell in which we can generate an EMP force $\vec{F}$ by maintaining a current density $\vec{J}$ between electrodes E_1 and E_2 in the presence of a transverse magnetic field $\vec{B}$. If the conductivity σ of the electrolyte increases, for instance in the downward direction, so will the current density $\vec{J}$ maintained by the potential difference V between the electrodes. Thus, the electromagnetic force density $\vec{F} = [\vec{J} \times \vec{B}]$ will increase with the conductivity σ in the direction of grad σ. We are at liberty to determine the direction of the $\vec{F}$ vector by choosing the direction of the current and of the magnetic field. Let us assume that the force $\vec{F}$ points downward (opposite to the direction shown in Fig. 6). We have now an analogue to a stable density gradient in the gravitational field where the weight density ($\vec{dg}$) is replaced by the electromagnetic force density $[\vec{J} \times \vec{B}]$. Since the direction of $\vec{F}$ points in the direction of increasing $[\vec{J} \times \vec{B}]$ values, the gradient is a stable one. If we were to reverse $\vec{J}$ or $\vec{B}$, we would invert the direction of $\vec{F}$ (as depicted in Fig. 6) and an unstable conductivity gradient would result comparable to a density gradient in which the density is increasing in the upward direction. By adding such an electromagnetically stabilized conductivity gradient to a density gradient, we can obtain a combined gradient of far greater stability[24].

The stability as well as destabilization of such a hybrid gravitationally–electromagnetically stabilized gradient can be demonstrated experimentally[24]. Fig. 7 shows four photographs of the transilluminated cell of Fig. 6. The fluid in the cell is filled with a solution in which a density gradient of a urea solution is accompanied by a conductivity gradient due to non-uniformly dissolved NaCl. The concentration of both solutes increases in the downward direction and, hence, both solutes contribute to the generation of a stable density gradient. In photograph A, the stability of the density gradient is enhanced by turning on a current of 0.5 A per cm^2 of electrode area. The intensity of the transverse magnetic field is 6,000 gauss. (Both, the current

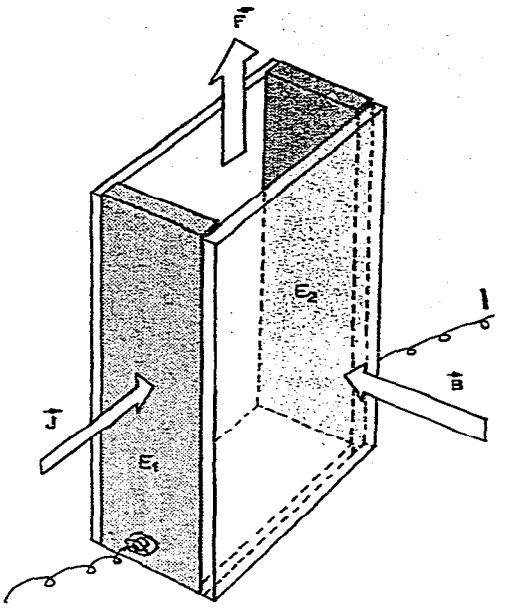

Fig. 6. Electromagnetophoresis cell. $\vec{J}$, Current density; $\vec{B}$, magnetic flux density; $\vec{F}$, electromagnetic force density; E_1 and E_2, electrodes. [From A. Kolin, *Biochim. Biophys. Acta*, 32 (1959) 538.]

and magnetic field are in phase, and sinusoidal of 60-Hz frequency. The above figures are r.m.s. values). The two gradients stabilize the liquid column against thermal convection which the high current density tends to engender. When we now reverse the current (*i.e.* its phase), we reverse the direction of the F vector, which now points upward as in Fig. 6. The configuration of the electromagnetic force density gradient is now unstable, while the stabilization by the density gradient is preserved.

To assess the combined action of the two gradients, we must add the gravitational and electromagnetic force densities at every point.

$$\vec{F} = (\vec{dg}) \pm [\vec{J} \times \vec{B}] \tag{4}$$

where $\vec{dg}$ is the gravitational force density (weight density) whose (downward) direction we designate as positive; $[\vec{J} \times \vec{B}]$ is the electromagnetic force density which can point up or down, depending on directions of $\vec{B}$ or $\vec{J}$. Since $\vec{J} = \sigma(\partial V/\partial x)$ (where $\partial V/\partial x$ is the potential gradient in the solution), we can write for eqn. 4

$$F = (dg) \pm B\,(\partial V/\partial x)\sigma \tag{5}$$

The stability thus depends on the gradient

$$\frac{\partial F}{\partial y} = g\left(\frac{\partial d}{\partial y}\right) \pm B\left(\frac{\partial V}{\partial x}\right)\left(\frac{\partial \sigma}{\partial y}\right) \tag{6}$$

(where $\partial V/\partial x = \text{const.}$).

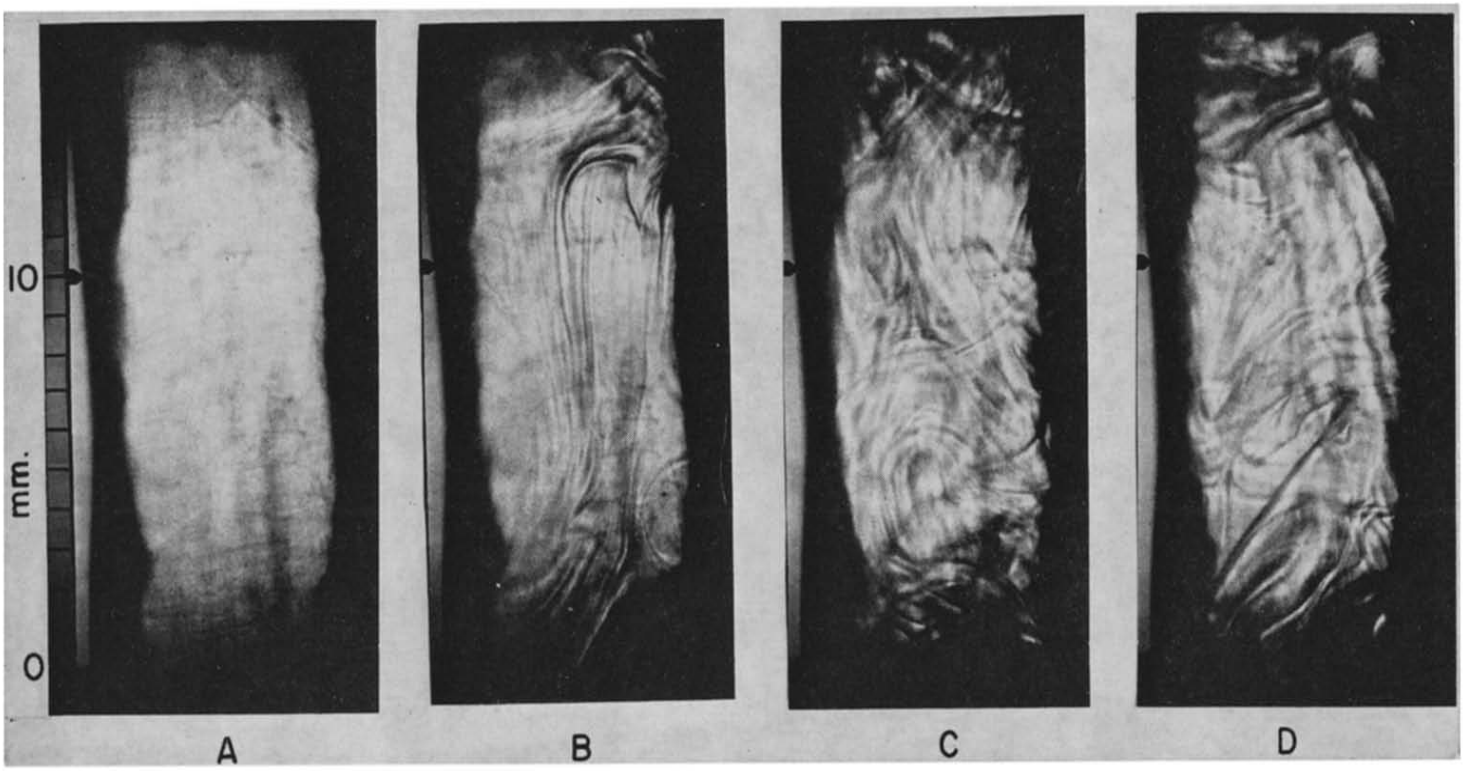

Fig. 7. Stabilization and destabilization of a density gradient by a superimposed conductivity gradient in a transverse magnetic field. (A) Stabilization of density gradient column reinforced by conductivity gradient in a suitably oriented (phased) magnetic field. (The electromagnetic force points in the directions of the density- and conductivity-gradients). (B), (C) and (D) The direction of the electromagnetic force is reversed by reversing the magnetic field or current. The electromagnetic force is now pointing in the direction of diminishing density and conductivity. The fluid column is destabilized as evidenced by turbulence revealed by "Schlieren" seen in photographs. [From A. Kolin, *Biochim. Biophys. Acta*, 32 (1959) 538.]

If in our concentration gradient where d and σ increase in the downward direction $\partial F/\partial y$ is positive (*i.e.* points downward), the resultant force density increases in the direction of the gravitational and electromagnetic forces in our example and the fluid column is stabilized. If the concentration distribution and the sign of the second term of equation (6) are such that $\partial F/\partial y = g(\partial d/\partial y) \pm B(\partial V/\partial x)(\partial\sigma/\partial y) = 0$, there is no stabilizing gradient. Finally, if the electromagnetic force $[\vec{J}\times\vec{B}]$ points in the direction of diminishing conductivity in our conductivity gradient (*i.e.* the second term of eqn. 6 is negative) and the absolute value of the negative second term of eqn. 6 surpasses the value of the first term, the column becomes unstable for $g\,|\,(\partial d/\partial y)\,| < |\,B(\partial V/\partial x)(\partial\sigma/\partial y)\,|$. Such a destabilization can be achieved by reversing the current or the magnetic field in an appropriately prepared combined g, σ gradient column.

It is worth adding that the surface of electrodes E_1 and E_2 of the cell in Fig. 6 could be coated with a very thin dielectric coating which would permit passing an alternating current of suitably high frequency between the electrodes without creating a short circuit precluding passage of a vertical direct current through the cell.

6. MAGNETOHYDRODYNAMIC CONVECTION—ENDLESS FLUID BELT ELECTROPHORESIS

6.1. Background of this development

Establishing density and/or conductivity gradients in the migration cell for stabilization against thermal convection introduced experimental and theoretical complications which I did not like. A stabilization method which I published in 1954[17], although mechanically more complicated, offered the possibility of performing electromagnetophoresis and electrophoresis in a fluid of uniform density. It involved rotation of a cell similar to that shown in Fig. 2 about a centrally located horizontal axis. This approach was based on the insight that thermal convection is a gravitational phenomenon and would not exist in a gravity-free space[17,25]. A particle entrained in a rotating cell will behave as if it were exposed to a rotating rather than unidirectional gravitational field. It will orbit with respect to the cell in a small circle about a stationary center instead of sedimenting to the cell bottom. A fluid element whose density is changed above the density of the ambient fluid by a temperature rise is analogous to a suspended particle and will be similarly inhibited from performing a unidirectional motion which would lead to thermal convection. It was thus possible to suppress thermal convection in such a cell rotating at a frequency of 1.3 r.p.s. while the NaCl solution was heated at the center of the cell by a current of 3 A passing between two electrodes 4 mm apart[17]. The rotation of the cell solved two additional problems in electromagnetophoresis: (1) it became unnecessary to adjust the density of the fluid to maintain particles in suspension and (2) the rotation of the cell within the magnetic field averaged out spatial variations in the field strength to which different portions of the cell were subjected, thus diminishing disturbances due to electromagnetic convection[18].

On my trip to Sweden in 1958 I saw an impressive independent development. It was Hjertén's rotating-tube electrophoresis apparatus in which rotational inhibition of thermal convection permitted obtaining beautiful electrophoretic zonal mobility spectra in the absence of stabilizing gradients[26]. Upon my return to Los Angeles, I

attempted to use the electromagnetic propulsion of my 1936 pumping experiment to replace the mechanical rotation of Hjertén's horizontal tube by electromagnetic rotation of the fluid in a stationary tube but failed to get satisfactory results. However, these experiments were not a total failure since they stimulated the following idea for stabilization against thermal convection in continuous-flow electrophoresis[11,25,27,28].

6.2. Principle of the method

Fig. 8a shows in cross-section an annular fluid volume sandwiched between two horizontal cylinders. The temperature of the inner cylinder is higher than that of the outer one. The resulting horizontal temperature gradient in the mid-plane of the annulus will tend to produce vortical fluid motion as indicated by a solid loop with arrows on the right side. The warmer fluid at the inner cylinder, being less dense will move upward while the denser fluid near the outer cylinder will move downward.

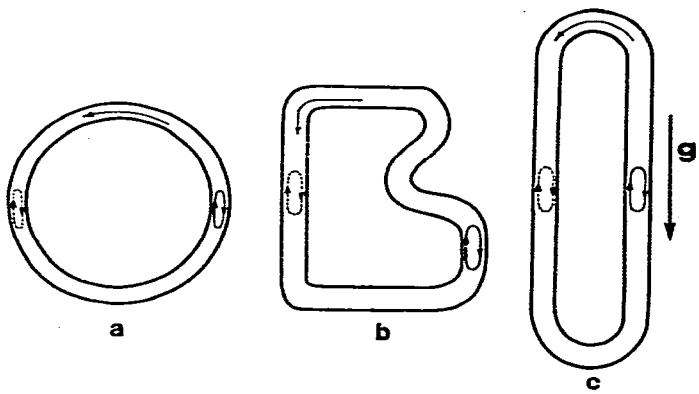

Fig. 8. Inversion of thermal convection vortices by fluid circulation in horizontal annular channels of different cross-sections (a, b and c). *g*, Gravitational field intensity. [From A. Kolin, in N. Catsimpoolas (Editor), *Methods of Cell Separation*, Plenum Publ. Co., 1977.]

Imagine now that we succeed in rapidly rotating the fluid in the annulus by 180° as indicated by the top arrow in the annulus. This will transfer our "solid" vortex into the position indicated by the dashed arrowed loop on the left annulus side. Due to inertia the fluid in the vortex near the inner cylinder will move downward and in the outer part of the vortex upward. These two directions of motion are, however, now opposite to the gravitational forces which generated the vortex and which still act on the fluid in it in the same directions; namely, upward on the warmer and specifically lighter fluid near the inner cylinder and downward on the cooler and specifically heavier fluid near the outer cylinder. Thus, the same forces which engendered the vortex on the right hand side of the annulus will retard and stop its rotation on the left hand side if we leave it there long enough. Since a certain amount of time is required to endow a vortex with its rotational kinetic energy, it is clear that we could effectively inhibit formation of thermal convection vortices by a slow uniform circulation of the fluid in the annulus as indicated by the top curved arrow.

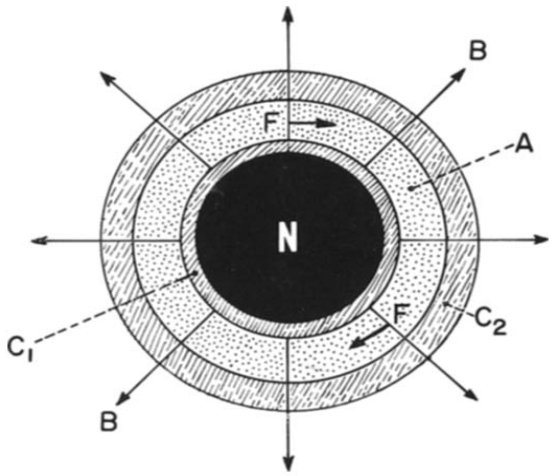

Fig. 9. Radial magnetic field (B) surrounding a cylindrical magnetic north pole (N) inside a buffer-filled annulus (A). C_1 and C_2, Walls confining the fluid in annulus A; F, electromagnetic force generated in the presence of a current flowing through fluid in A at right angles to the page. [From A. Kolin, in N. Catsimpoolas (Editor), *Methods of Cell Separation*, Plenum Publ. Co., 1978.]

It is obvious that the closed circulation path of the fluid need not be circular, but could have arbitrary shapes as those shown in Figs. 8b and 8c. It remains now to find a way to maintain such constant fluid circulation. Such a scheme is illustrated in Fig. 9. N represents in cross-section an isolated cylindrical magnetic north pole

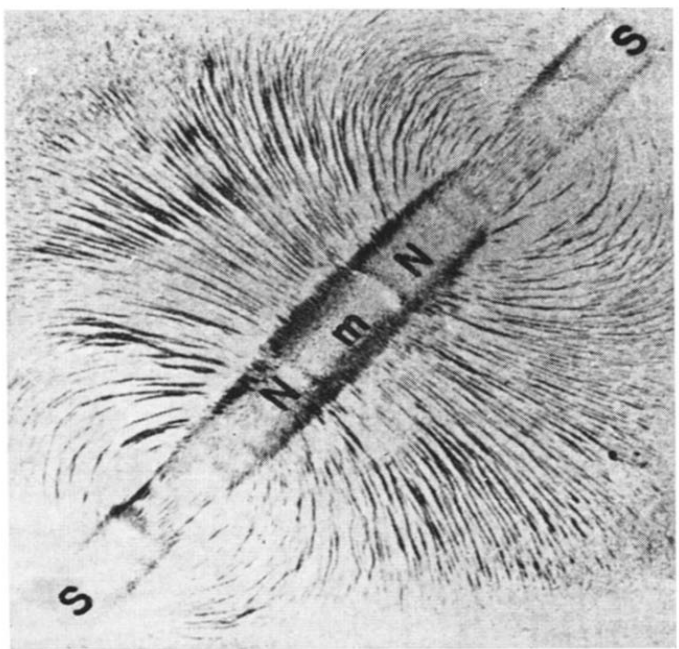

Fig. 10. Magnetic field distribution about a cylindrical soft-iron core m located between oppositely oriented cylindrical bar magnets (N, S). [From A. Kolin, *J. Chromatogr.*, 26 (1967) 164.]

and the vectors $\vec{B}$ its field lines. The pole is surrounded by two concentric plastic cylinders C_1 and C_2 between which is sandwiched an annular electrolyte volume. If we now imagine an electrical current passing through the electrolyte in the direction from the reader into the page, tangential electromagnetic forces (indicated by vectors $\vec{F}$) will be exerted upon the electrolyte, and the fluid in the annulus will be set into a very constant circular motion.

Since there are no isolated magnetic poles in nature, we must devise an approximation. Fig. 10 shows that a cylindrical soft-iron core m sandwiched between the north poles N of two cylindrical bar magnets NS exhibits a nearly radial magnetic field near its surface as is depicted in Fig. 9.

6.3. The circular endless belt apparatus

Fig. 11 translates this scheme into a simple instrumental arrangement. The magnets and iron core M are held inside the inner plastic cylinder C_1 which is surrounded by an outer plastic cylinder C_2 leaving an annular gap of 1.5 mm between them. The plastic cylinders are cemented to the electrode compartments EC_1 and

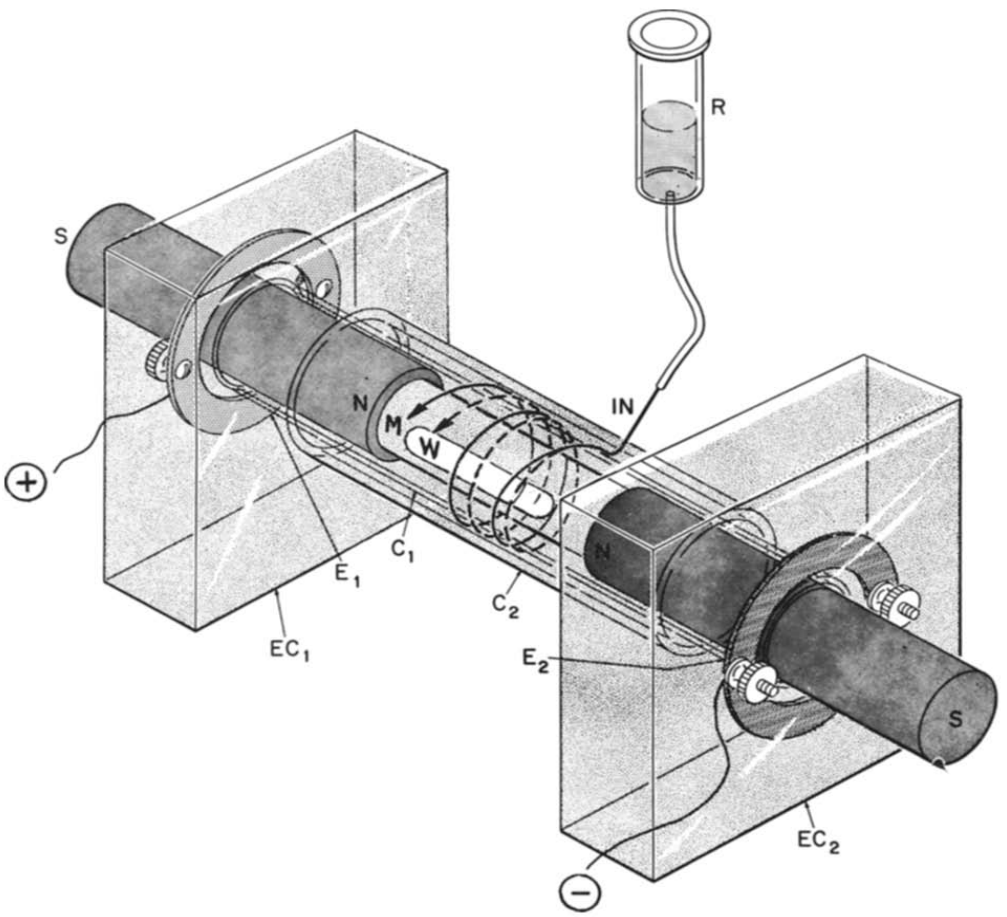

Fig. 11. Scheme of circular endless belt electrophoretic separator. N and S, magnet poles; M, soft-iron core; W, window in core M; C_1 and C_2, concentric plastic cylinders; EC_1 and EC_2, electrode compartments; E_1 and E_2, electrodes; IN, injector; R, sample reservoir. [From A. Kolin, *J. Chromatogr.*, 26 (1967) 164.]

EC_2 so that the latter communicate with each other through the annulus between C_1 and C_2. E_1 and E_2 are electrodes mounted in the compartments EC. If we now pour buffer solution into the cell and connect E_1 and E_2 to a current source, the interaction between the radial magnetic field and the axial current will cause the buffer in the annulus to rotate with clocklike regularity.

R is a reservoir containing the solution or suspension to be subjected to electrophoretic analysis. It delivers its contents through a fine glass capillary which passes through cylinder C_2 and terminates in the middle of the annular gap. If we inject, for instance, electrically neutral particles, they will be entrained in the circulating fluid and will accumulate in a circular orbit (in the absence of electro-osmosis). If on the other hand the particles are negatively charged, they will combine circular motion with axial electrophoretic migration toward the anode and their path will be a left-handed helix as shown in Fig. 11. The helical pitch is a measure of the electrophoretic mobility of the particles. Two ions or particles differing in electrophoretic mobility will follow divergent helical paths of different pitch as shown by the solid and the dashed helix in Fig. 11. Positive particles will migrate toward the cathode in a right-handed helical path. The window W is a gap in the soft-iron cylinder which permits passage of light through the core. In this fashion particles like cells and cell organelles can be visualized and photographed by dark-field illumination.

6.4. The non-circular endless belt apparatus

The use of a circular annular path is not favorable, especially for cell separations. Fig. 12A shows how cell sedimentation can move the injected particle stream toward the cylinders to which they could become attached. This can be remedied by using a non-circular "racetrack" for the fluid circulation. The scheme is the same as shown in Figs. 9–11, except that the cross-sections of the magnets, iron core and plastic enclosures are no longer circular. In Fig. 12B the particles move mostly in a vertical path in the central plane of the racetrack. When they move to the left under the core they sediment slightly below the midline and continue their upward journey

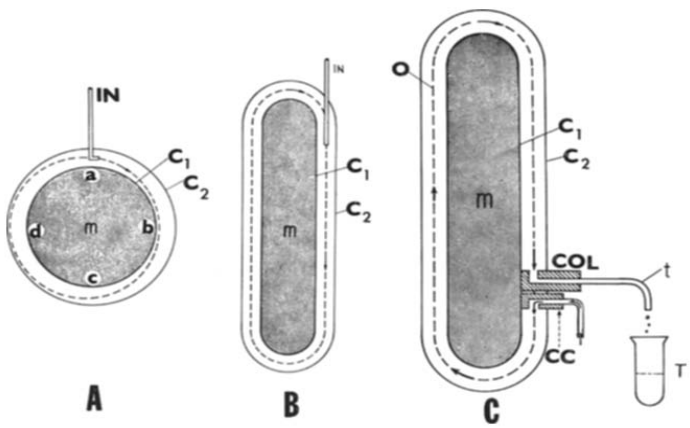

Fig. 12. Electromagnetic circulation of injected particles in annuli of different shapes. m, Iron core inside annulus; IN, injector; C_1 and C_2, walls confining fluid in annulus; COL, collector; t, collector tubing; CC, collector compensator; T, test tube. [From A. Kolin, in N. Catsimpoolas (Editor), *Methods of Cell Separation*, Plenum Publ. Co., 1978.]

left of the midline. However, as they move to the right above the core m, sedimentation brings them back toward the center of the racetrack so that they never get too far away from it. Fig. 12C illustrates how a collector COL can be installed at the end of the helical path to intercept the separated particles (or ions) and guide them to tubes T of a fraction collector.

Fig. 13 illustrates the separation space of the apparatus in a perspective drawing. The iron core C (insulated with a layer of about 0.2 mm thickness of Epoxylite) harboring a quartz window W is centered (by small plastic spacers) with the mantle MA so that a gap of 1.5 mm between them surrounds the core C. The buffer solution which fills this non-circular annular gap is the endless fluid belt in which the continuous-flow electrophoretic separation takes place. Four permanent Alnico bar magnets of which only the N poles are shown generate the magnetic field which traverses the annular buffer belt substantially at right angles. The electrical current flows through the annulus in the direction of the arrows seen inside the tubes CP. The interaction of this current with the magnetic field maintains the buffer belt in a uniform circulation around the core C. The hollow core C is cooled by water entering and leaving through the cooling water pipes CP. The core thus cools the buffer belt from the inside. The outside of the buffer belt is also cooled. This is accomplished by milling out the front and back walls of the mantle MA leaving a thin plastic membrane to confine the buffer belt on the outside. Cooling water is circulated

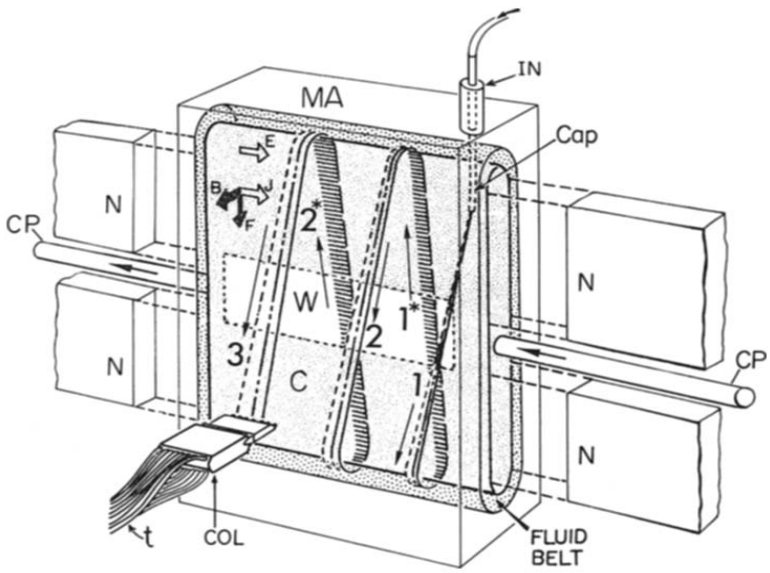

Fig. 13. Electrophoretic separation space of non-circular endless belt apparatus. N, north poles of magnets; C, hollow iron core; CP, cooling pipes carrying cooling fluid circulating through C; W, window in C; MA, mantle surrounding annulus (fluid belt); IN, injector; Cap, capillary; COL, collector; t, collector tubing; $\vec{E}$, electric field vector; $\vec{B}$, magnetic field vector; $\vec{J}$, current density vector; $\vec{F}$, electromagnetic force vector. 1* and 2*, first and second ascending streaks (behind the core C). 1, 2 and 3, first, second and third descending streaks (in front of the core C); L, light beam passing through the bottom of the annulus. [From A. Kolin, in N. Catsimpoolas (Editor), *Methods of Cell Separation*, Plenum Publ. Co., 1978.]

through the hollow cooling chambers thus produced in the mantle walls and cools the buffer belt by outward heat flow across the thin plastic membranes.

The sample of the material to be subjected to electrophoresis is injected at the center of the annular buffer belt thickness through a capillary of the injector (IN). The electrophoretically distinct components migrate in trajectories of different helical pitch and are intercepted at the end of their path by collector COL from which tubes t guide them to different test tubes.

6.5. Omission of membranes

While Fig. 13 shows the endless fluid belt and the magnets, it does not show the connection between the endless belt and the buffer and electrode compartments. This connection is illustrated in Fig. 14 which does not show the magnets and the core. The separation chamber shown in Fig. 13 is the section SCH of Fig. 14. In addition to the window W in the core there are two windows in the mantle, one in front and another one behind the core window. The electrodes E_1 and E_2 are in electrode chambers EC which are separated from the buffer chambers BC by plates P whose lower portions are perforated (as indicated by dashed lines). This is an

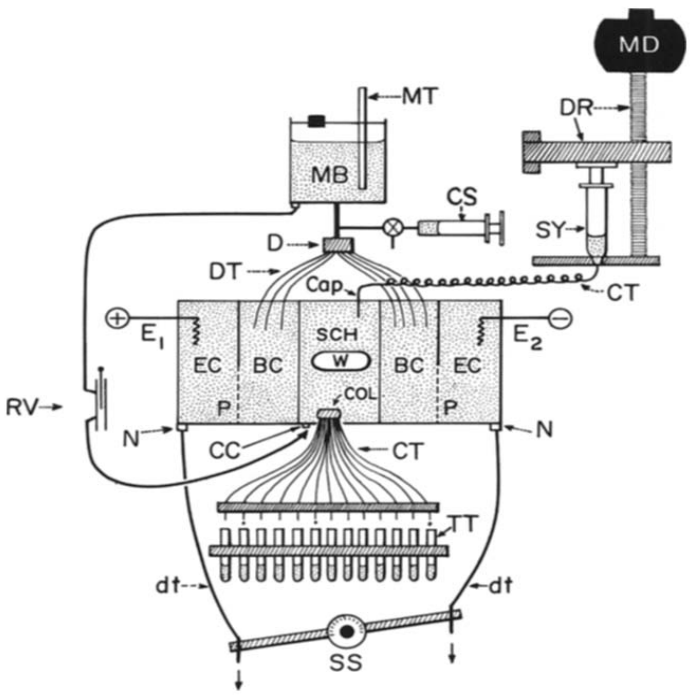

Fig. 14. Scheme of endless belt apparatus flow system. SCH, separation chamber; W, window; Cap, injector capillary; COL, collector; CT, collector tubing; CC, collector compensator nipple; TT, test tubes; BC, buffer compartments; EC, electrode compartments; E_1 and E_2, electrodes; N, nipples of rigid drainage tubes (not shown); dt, narrow plastic drainage tubes; SS, "see-saw"; P, perforated plates; MB, Mariotte bottle; MT, tube of Mariotte bottle; CS, clean-out syringe; D, distributor; DT, distributor tubes; CT, coiled tubing linking capillary to sample syringe; SY, sample syringe; MD, motor drive; DR, screw and plate which drive the plunger of syringe SY; RV, regulator valve for control of collector compensator inflow. [From A. Kolin, in N. Catsimpoolas (Editor), *Methods of Cell Separation*, Plenum Publ. Co., 1978.]

important distinguishing feature between the endless fluid belt apparatus and the free-flow electrophoresis apparatus[9,10], where the electrode chambers and the separation chamber must be partitioned by membranes to permit maintenance of a vertical pressure gradient in the separation chamber to drive the buffer through it. The electromagnetic propulsion does not require such a pressure gradient and thus permits omission of the membranes.

The significance of the omission of the membranes is as follows. The perforations in the plates P make it possible to prevent electrolysis products from migrating from the compartments EC into the separation chamber SCH. This is achieved by centrifugal buffer flow. Buffer is delivered into both buffer compartments BC at a constant pressure head from Mariotte bottle MB via distributor D through thin plastic tubes DT. This creates a rapid buffer flow through the small perforations in the plates P directed from the chambers BC toward the chambers EC so that when this flow is fast enough the electrolysis products cannot migrate toward the chamber SCH. This avoids spatial and temporal variations in pH and conductivity in the annular separation space which can be caused by membranes. The centrifugal buffer flow idea was first applied by Bergrahm to a column electrophoresis apparatus[29]. It was subsequently adapted to endless belt electrophoresis[12,30].

6.6. Axial buffer flow

In addition to the symmetrical centrifugal buffer flow, the scheme of Fig. 14 permits the imposition of an axial buffer flow through the annulus. This can be accomplished in step-wise fashion by transferring some of the tubes DT from the left to the right buffer chambers BC or vice versa. Usually one employs a surplus of tubes in the right BC chamber to maintain an axial buffer flow from right to left. A fine-control of axial buffer flow is accomplished by means of the "see-saw" SS which permits to lower the left outflow tube dt as the right one is raised, or *vice versa*. The collector compensator CC allows to return to the separation chamber (under the collector COL) an amount of buffer which enters the collector from the top. The clean-out syringe CS permits removal of air bubbles from the distributor system. The motor MD and drive DR expell the fluid to be analyzed from the syringe Sy via the tubing CT and capillary Cap into the endless buffer belt. A more detailed description of the instrument and its performance will be found elsewhere[31].

6.7. Illustrations of the performance of the circular endless belt apparatus

The following photographs illustrate the performance of the simple circular-path separator shown in Fig. 11. Typically the diameter of the annulus is about 3 cm, the annulus thickness 1.5 mm, the period of revolution of the buffer is about 22 sec at a current density of 10^{-2} A/cm^2 and magnetic field intensity of 150 gauss. Visible separations can be frequently seen within 5–10 sec[11].

Fig. 15 illustrates 15 helical turns of erythrocytes visualized by dark field illumination of the particle path through window W of Fig. 11[27].

Fig. 16 shows the separation of two microorganisms: *Saccharomyces cerevisiae* and *Rhodotorula*. Four consecutive helical turns are seen .The duration of migration from turn to turn is about 20 sec. We see how the separation between the particles gains equal increments with each turn[27].

Fig. 17 demonstrates an important stability property of the endless belt system.

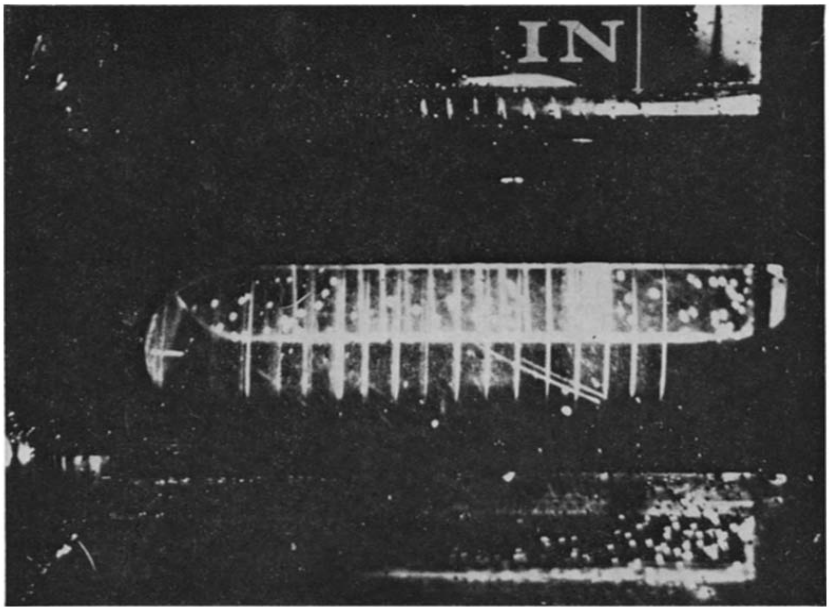

Fig. 15. Visualization by light scattering of a 15-turn streak of erythrocytes in circular endless belt. IN, Injector; W, window in core of central iron cylinder. The illumination is directed toward the reader (forward scattering). [From A. Kolin, *J. Chromatogr.*, 26 (1967) 164.]

The photos show several helical turns of the dye Evans blue: (a) at a voltage of 75 V between the cell electrodes and (b) after raising the voltage to 150 V. We see that the helical pitch has not changed although the electrophoretic migration speed has been doubled! The reason is the concomitant doubling of the rotational speed which allows only half the time for migration between the consecutive turns. In (c) the buffer has been diluted 1:2 to lower the electrical conductivity of the buffer while maintaining the same current (25 mA) as in experiment (a). The helical pitch is about doubled, because the voltage across the cell had to be increased while the constancy of current insured a constant rate of buffer rotation[11].

The separation between two components of a mixture increases with each helical turn, as we can see from Fig. 16. There is, however a limitation in this advantage since eventually the faster component after n turns my approach coincidence with the slower component of the $(n+1)$st turn. Such a fusion of previously well resolved components can be avoided by superimposing a lateral buffer flow in the direction of electromigration upon the electrophoretic migration. One can thus increase the helical pitch to any desired value and make wider separations possible. Fig. 18 illustrates changes in helical pitch by imposed lateral buffer flow. Initially, in (a), there is no lateral buffer flow. In (b) a lateral flow from right to left is initiated with consequent increase in pitch and in (c) the lateral flow is increased further[27].

Conversely, one can impose the lateral streaming in the direction opposite to electromigration. In this case one can obtain a non-isoelectric accumulation of a given component in a circular orbit. In Fig. 19 we see in (a) the initial helix of india ink. A lateral streaming arresting the right-to-left migration of india ink has been

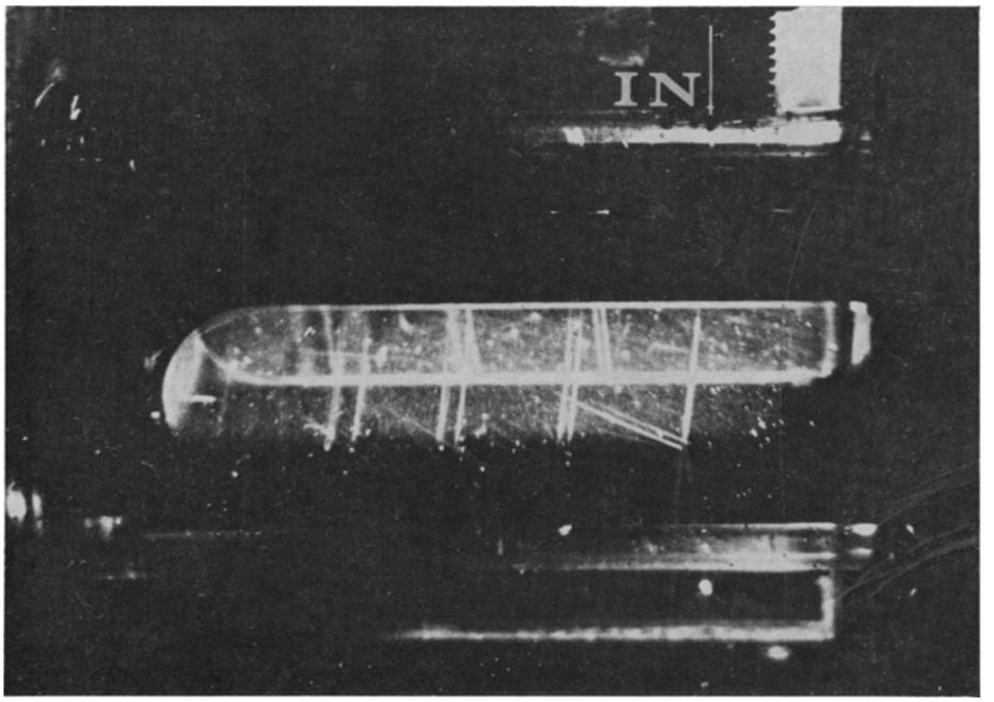

Fig. 16. Separation of two micro-organisms *Rhodotorula* and *Saccharomyces cerevisiae*, visualized by dark-field illumination. a, b, c, d, Consecutive helical turns; IN, injector. Arrow marks the point of sample injection. W, window in iron core. [From A. Kolin, *J. Chromatogr.*, 26 (1967) 164.]

imposed in Fig. (b) and the particles are accumulated in a circular orbit under the arrow[27].

Under certain conditions it may be advantageous to collect different electrophoretic components after a different number of turns. For instance, suppose we have 3 components of which the two faster ones are clearly resolved and get into different collector tubes, while the slowest component is so close to its neighbor that some of it enters the collector tube which intercepts its faster neighbor. Under these circumstances we can adjust the lateral flow so that the slowest component just misses the collector after n turns while its faster neighbors are intercepted by it in the nth turn. The slowest component then migrates one more turn and enters the collector in the $(n+1)$st turn ahead of the faster components and a considerable distance away from them in the collector[27].

Endless belt electrophoresis is not limited to continuous preparative separations. Discontinuous zone separations can be performed for micro-analysis. For this purpose we can inject a very fine streak (about 100 μm in diameter or less) of a mixture to be analysed. The streak may be as short as 1 cm or less and thus comprise a volume smaller than 0.1 μl. We can impose a lateral streaming to place the electrophoretically slowest zone into a stationary circular orbit allowing the faster components to migrate to the left until all components can easily be separated. The separate collection of the zones can be achieved by increasing lateral streaming so as to intercept the helical paths of the zones by the collector.

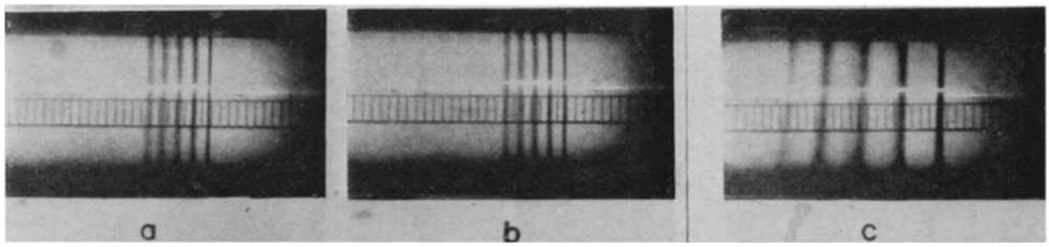

Fig. 17. Effect of voltage on helical pitch in circular endless belt apparatus. (a) Helix of Evans blue obtained at a current of 25 mA and a voltage of 75 V between the electrodes. (b) Helix of Evans blue after raising the voltage to 150 V. (c) Change in helical pitch at the current used in (a) after diluting the buffer 1:2. [From A. Kolin, *Proc. Nat. Acad. Sci. U.S.*, 46 (1960) 509.]

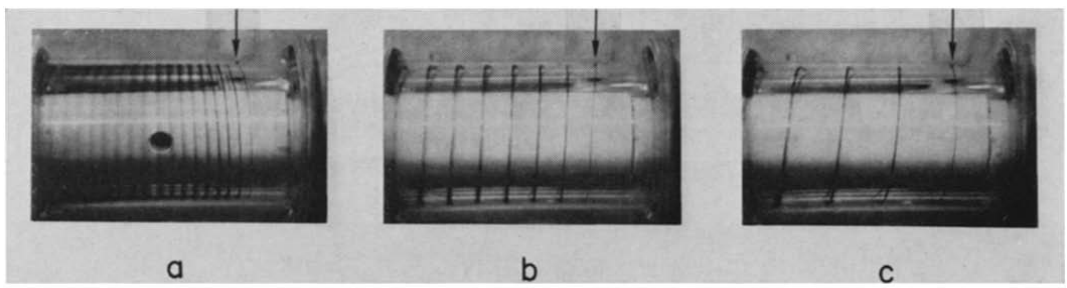

Fig. 18. Effect of lateral flow on helical pitch. The lateral flow is from right to left. The arrow marks the entry point of sample. The rate of lateral flow is increasing as we progress from (a) to (c). [From A. Kolin, *J. Chromatogr.*, 26 (1967) 164.]

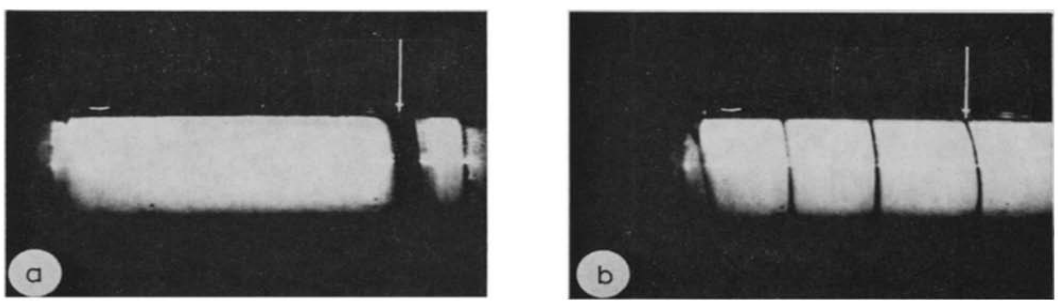

Fig. 19. Non-isoelectric accumulation in stationary orbit. (a) Helix of india ink injected at arrow. (b) Lateral flow is adjusted to accumulate india ink in a zero-pitch helix, *i.e.* circular orbit. [From A. Kolin, *J. Chromatogr.*, 26 (1967) 164.]

6.8. Illustrations of the performance of the non-circular endless belt apparatus

The dimensions of the annulus of the non-circular endless belt are about 10 cm in height, 9.5 cm in lateral length and 1.2 cm in width determined by the thickness of the iron core. The circumference of the racetrack is about 21 cm. The non-circular vertical endless belt is more effective than the circular one, not only with particles by inhibiting their sedimentation, but also with macromolecular solutions which can be injected at higher concentration without the hazard of the injected dense streak sedimenting excessively toward the walls of the core and mantle. The racetrack is long enough to yield adequate separations after the minimum

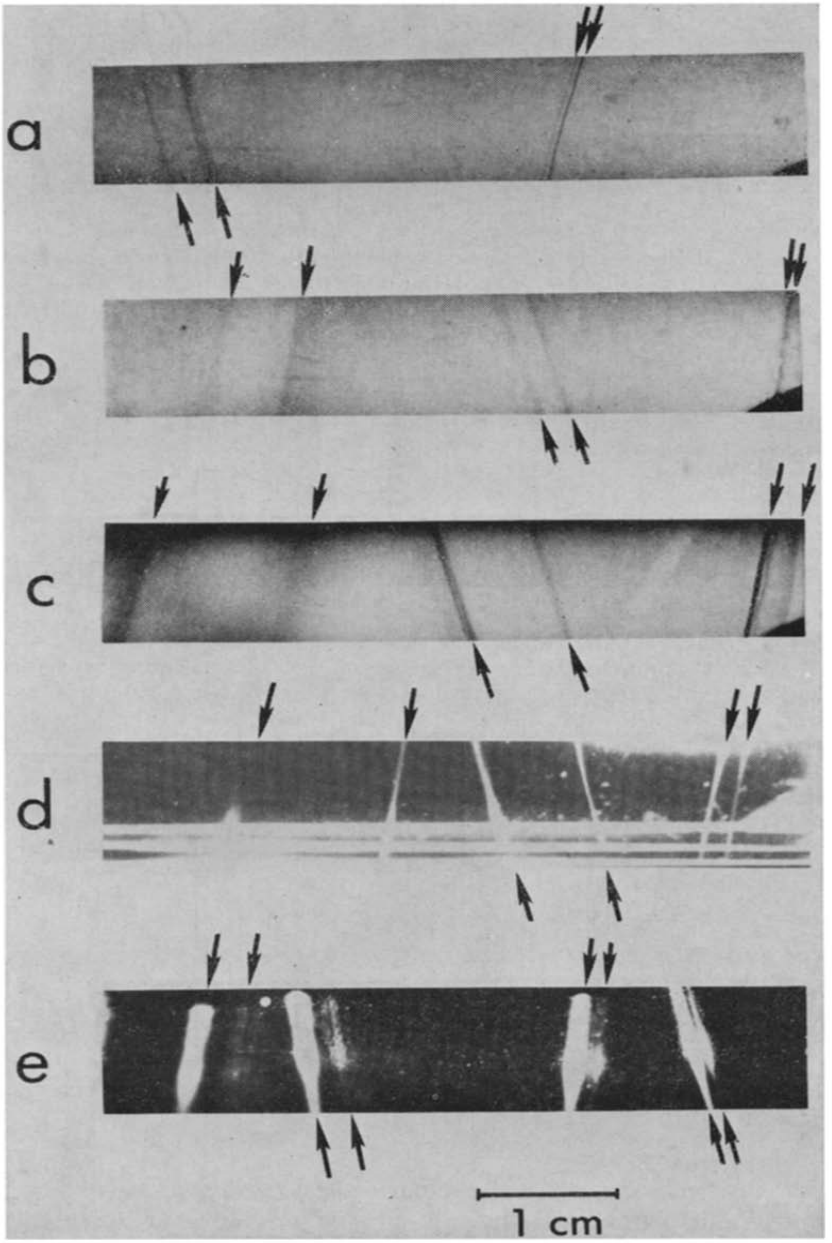

Fig. 20. Streaks in endless belt electrophoresis apparatus photographed (a) and (b) by ultraviolet light, (c) by visible light absorption, and (d) and (e) by light scattering. Current was 150 mA in (a) and 200 mA in all the others. (a) TMV strains U1 (left) and U2 (right), pH 7.1. (b) Human serum proteins, albumin (left) and γ-globulin (right), pH 8.75. (c) Mixture of bovine hemoglobin (left) and horse heart cytochrome c (right), pH 9.3. (d) *Rhodotorula* sp. (left) and *Escherichia coli* (right), pH 7. (e) Erythrocytes (left) and mainly granulocytes (right), pH 7.1. The streak pattern descending from the injector is out of the field of view. [From A. Kolin and S. J. Luner, *Anal. Biochem.*, 30 (1969) 111.]

number of $1\frac{1}{2}$ revolutions. It is seldom that more than $2\frac{1}{2}$ revolutions are required in practice.

The following figures illustrate the effectiveness of the vertical non-circular endless belt electrophoretic separator. Fig. 20 illustrates separations of blood cells, fungi, bacteria, viruses and macromolecules (proteins)[12]. In Fig. 20a we see the first descending and the first ascending portions of the non-circular helical paths of two strains of tobacco mosaic virus (electrophoresis proceeds from right to left). The higher-mobility strain U1 is less abundant than the slower migrating strain U2 in the mixture. The separation seen in the first double streak was achieved about 8 sec after injection into the annulus and the 3-mm separation seen in the second double streak on the left resulted after *ca.* 0.5 min electromigration. The mobility difference between these virus strains was 15 TU. They were visualized by ultraviolet photography which was also used to photograph the separation between human serum albumin (left streak) and γ-globulin (right streak) shown in Fig. 20b.

Visible-light photography was used to record the separation of a mixture of bovine hemoglobin (left streak) and horse heart cytochrome *c* (right streak) into two streaks shown in Fig. 20c.

The splitting of a mixture of the yeast *Rhodotorula* (left) and *Escherichia coli* (right) seen in Fig. 20d was visualized by dark-field illumination as was the separation of erythrocytes (faster component) and granulocytes (slower component) illustrated in Fig. 20e.

Fig. 21 shows a rapidly achieved (about 50 sec) wide separation pattern of a mixture of 3 bacteria: *E. coli*-ML35 strain (a), *Proteus vulgaris* (b) and *E. coli*-BE30 strain (c). It is interesting to note that *Proteus vulgaris* splits into two electrophoretically distinct components b_1 and b_2.

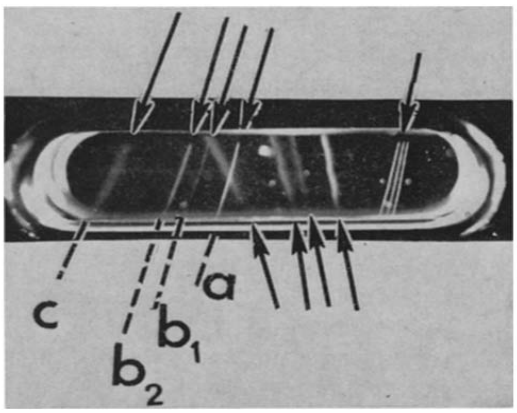

Fig. 21. Separation of 3 bacteria with endless belt. (a) *E. coli*-ML35 strain. (b_1) and (b_2) Two components of *Proteus vulgaris*. (c) *E. coli*-BE30 strain. [From A. Kolin, in N. Catsimpoolas (Editor), *Methods of Cell Separation*, Plenum Publ. Co., 1978.]

Finally, in Fig. 22 we see the separation of mouse mesenteric lymph node cells into two electrophoretically distinct components.

The main usefulness of endless belt electrophoresis lies in the field of particle separations which could not be carried out very effectively and conveniently by

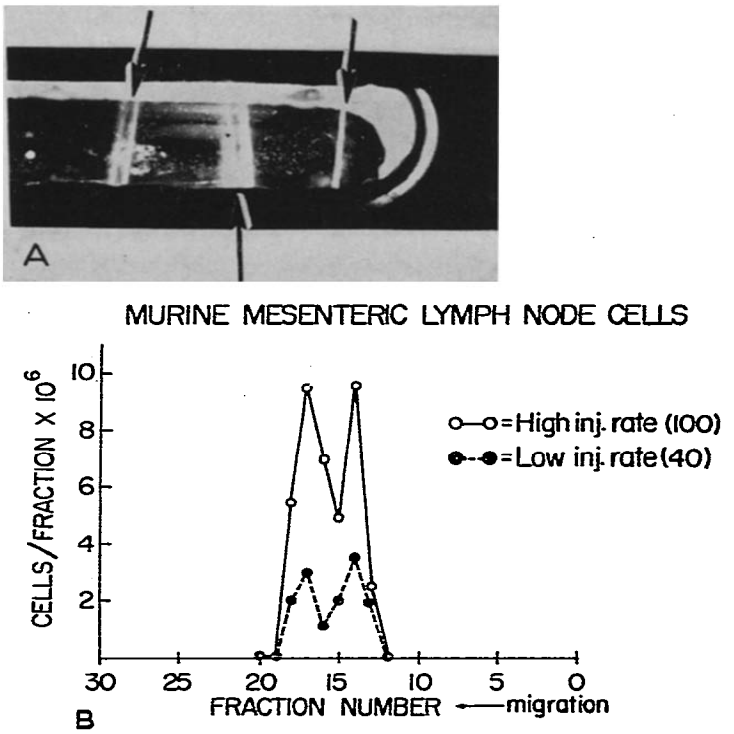

Fig. 22. Separation of murine mesenteric lymph node cells into two components. A, Photograph of separation pattern; B, collection patterns at high and low sample injection rates. [From A. Kolin, in N. Catsimpoolas (Editor), *Methods of Cell Separation*, Plenum Publ. Co., 1978.]

electrophoresis in supporting media. Although endless belt electrophoresis of macroions is very convenient, it cannot compete with the resolving power of gel electrophoresis.

6.9. Resolving power

The theory of resolution in endless belt electrophoresis and free-flow fluid curtain deviation electrophoresis is essentially the same. It has been worked out for endless belt electrophoresis[28] and utilized by workers using fluid curtains[10,32]. We shall proceed therefore for simplicity as if we were dealing with a flat fluid sheet and make reference to the shape of the endless belt only wherever it is necessary.

In the preceding discussion we were tacitly assuming a uniform flow of buffer in the fluid belt and absence of electro-osmosis. Under such unrealistic ideal conditions and in the absence of diffusion the resolution criterion is self-evident. An injected streak of circular cross-section containing two separable components will simply split into two streaks which will be considered as resolved as soon as they no longer overlap. Actually, the curtain flow velocity profile is parabolic and an injected circular streak is distorted in cross-section as shown in the photograph of Fig. 23[30,33]. The photograph has been taken looking end-on at the helical streak of an endless belt apparatus as it turns over the top of the core C. The originally circular streak cross-section is distorted into a crescent-like shape. The electromigration is from

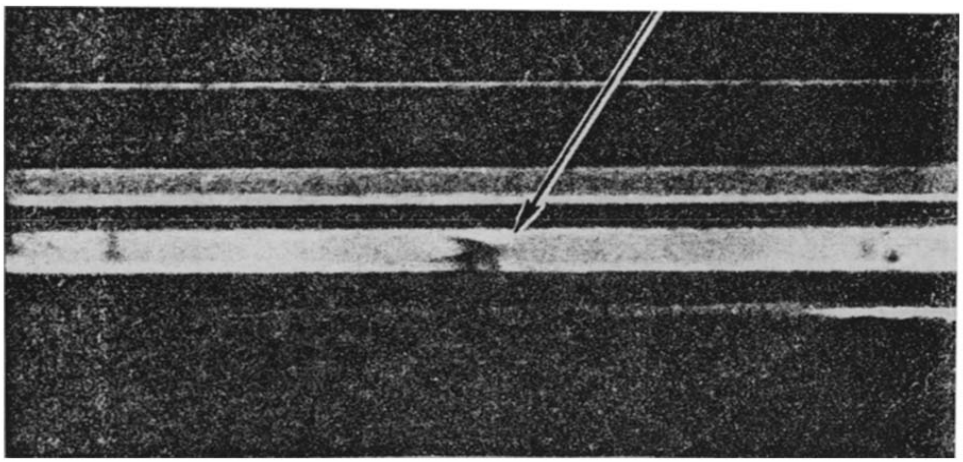

Fig. 23. "Crescent" distortion of an originally circular streak cross-section. End-on view of streak at the top of endless belt annulus. [From S. J. Luner, *Thesis*, Univ. of California, Los Angeles, Calif., 1969.]

right to left. Thus, the "horns" of the crescent contain particles which have advanced further to the left than those at the annulus center. As we shall see below, this does not mean that the electromigration velocity is smaller at the center than near the walls of the annulus.

We can visualize the process of streak distortion as follows. The white stripe in Fig. 23 at the center of which the crescent is located is the cross-section of the fluid curtain which we imagine flowing in the direction from the reader toward the page. Assume that a circular streak of negative particles starts its journey through the curtain at the eye level of the reader. They migrate to the left toward the anode as they move toward the page in the laminar flow within the fluid curtain. In view of the parabolic velocity profile in the laminar flow, the fluid velocity toward the page will be greatest at the center of the fluid curtain and will diminish toward zero at the walls. Therefore the centrally located particles will require less time than non-central particles to reach the plane of the page and will have been, consequently, migrating to the left a shorter time, than the particles near the walls confining the curtain. These particles will require a longer time to reach the plane of the page and, hence, will spend more time in electromigration to the left and will be deviated more in that direction. In view of the fact that this distortion results from the combination of the uniform electrophoretic velocity distribution of the particles with a parabolic flow velocity distrubution and because of the resulting divergence of the trajectories of the centrally located "rearguard" of the particle streak and of the outermost particles nearest the curtain walls, I called this phenomenon "parabolic divergence"[28,31]. This phenomenon has nothing to do with electro-osmotic streaming, in fact, the latter can be used to remove parabolic divergence so as to approximate ideal freedom from streak distortion, as we shall see below.

The distribution of the velocity u in the fluid curtain is

$$u = u_0 \left[1 - 4\left(\frac{z}{h}\right)^2\right] \tag{7}$$

where u_0 is the central maximum velocity, z is the distance of a point from the mid-plane of the curtain and h the thickness of the fluid curtain[11,28,31]. If we combine this vertical curtain flow with a transverse parabolic lateral flow v' (as it is used in the endless belt apparatus)

$$v' = v_0' \left[1 - 4\left(\frac{z}{h}\right)^2\right] \tag{8}$$

we obtain a resultant motion in which the fluid velocity will deviate from the vertical by the same angle of inclination i regardless of the value of z:

$$\tan i = \frac{v'}{u} = \frac{v_0'}{u_0} \cdot \frac{1 - 4\left(\frac{z}{h}\right)^2}{1 - 4\left(\frac{z}{h}\right)^2} = \frac{v_0'}{u_0} = \text{const.} \tag{9}$$

Since the coordinate z cancels out, an injected streak as thick as the fluid curtain will be deviated at all points of its cross-section by the same angle i and there will be no crescent distortion[28,31].

On the other hand, streak distortion will occur if the vertical flow represented by eqn. 7 is combined with a lateral motion of uniform velocity over the thickness of the curtain[28,31]. Since electro-osmosis is usually present under the experimental conditions of electrophoresis we shall include this fluid motion in our equation for horizontal particle velocity (in the absence of imposed lateral laminar flow). The electro-osmotic velocity (v) distribution is given by[11,31]

$$v = \frac{f_y}{2\eta}\left[z^2 - \left(\frac{h}{2}\right)^2\right] + v_w \tag{10}$$

In this equation f_y is the force density responsible for electro-osmotic streaming, η the fluid viscosity, and v_w the fluid velocity at the walls due to electro-osmosis. If we now add to this horizontal velocity the particle velocity due to electrophoresis $v_e = -\mu E$ (where μ is the electrophoretic mobility and E the electric field intensity), we obtain the resultant horizontal particle velocity

$$v^* = \frac{f_y}{2\eta}\left[z^2 - \left(\frac{h}{2}\right)^2\right] + E(W - \mu). \tag{11}$$

The term W is the electro-osmotic mobility, *i.e.* fluid velocity at the curtain wall at unit electrical field intensity and μ is the electrophoretic mobility of the particles.

The angle i of streak deviation will now be given by

$$\tan i = \frac{v^*}{u} = \left(\frac{f_y}{f_x}\right) \frac{z^2 - \left(\frac{h}{2}\right)^2}{z^2 - \left(\frac{h}{2}\right)^2} + \frac{E(W - \mu)}{z^2 - \left(\frac{h}{2}\right)^2} \tag{12}$$

or

$$\tan i = f_y/f_x + \frac{E(W-\mu)}{z^2 - \left(\frac{h}{2}\right)^2} \tag{13}$$

where f_x is the vertical force density responsible for maintaining the vertical curtain flow[11,31]. The coordinate z occurs now only in the right-hand term. We see that this term vanishes for $W = \mu$. The angle of streak deflection becomes then independent of z (ref. 11):

$$\tan i = f_y/f_x = \text{const.} \tag{14}$$

It was thus recognized in 1960 that the parabolic divergence (streak distortion) vanishes for one particular particle species, namely that particular electrophoretic component whose electrophoretic velocity equals the electro-osmotic velocity at the wall[11]. The streak corresponding to this particle species in an electrophoretic separation spectrum will be free of parabolic divergence, even if the streak diameter is as large as the thickness of the curtain. All the other components of the mixture will have streaks which will deteriorate by broadening[11].

This compensation phenomenon would not be very useful without the ability to change at will the electro-osmotic mobility W of eqn. 13. With this capability, one could adjust W to remove streak distortion from any electrophoretic component and optimally collect it in a wide streak. Such a possibility has been described in an ingenious suggestion[32] to modify in controlled fashion the average value of the wall zeta-potential. However, even if fully successful, this idea would permit in analysis of a mixture only one component at a time to be collected under favorable conditions. An entirely different approach offers the possibility of simultaneous streak collimation for all electrophoretic components and thus achievement of optimal resolution at maximal throughput[31,34,35].

6.10. Preparative resolution

We define the preparative resolving power R in streak deflection electrophoresis as the ratio between the mobility difference $\Delta\mu$ of two particle species which can be distinguished (and collected) as two separate components and the mean of their electrophoretic mobilities $\bar{\mu}$ (ref. 28):

$$R = \frac{\bar{\mu}}{\Delta\mu} \tag{15}$$

It has been shown[11] that the preparative resolution of the endless belt of thickness h as well as the free-flow curtain apparatus is given by

$$R = \bar{\mu}/\Delta\mu = (h/d)^2 \tag{16}$$

We can thus achieve any desired degree of resolution by making the streak diameter d suitably small[11]. For instance, by using an injector yielding a streak diameter $d = 0.15$ mm in a curtain or annulus of $h = 1.5$ mm thickness, we obtain from

eqn. 16 $\Delta\mu \approx 10^{-2}\,\bar{\mu}$ and we can resolve two ionic species differing by 1% in their electrophoretic mobilities.

In practice, where high throughputs are often essential one must make a compromise between the conflicting requirements of high throughput (thick streak) and high resolution.

6.11. Mobility measurements

The above considerations of resolving power apply only to preparative separations. In analytical applications like measurement of the electrophoretic mobility, streak distortion is not a problem. The central edge of the streak (the trailing edge in Fig. 23) is very sharp. If we confine our attention to this edge, we are dealing in effect with an infinitely thin well centered streak.

For mobility measurements in the endless belt one needs a baseline of zero mobility as a reference. This can be obtained by injecting an uncharged dye like Apollon whose streak provides such a baseline which is valid in the presence of electro-osmotic and lateral laminar streaming. For absolute mobility measurements, we inject a bolus of dye and measure the period of revolution. Then the deviation from the baseline streak of the streak of the particles whose mobility is being measured is determined after one revolution. This gives the absolute value of electrophoretic velocity. The electrical field intensity is obtained by measuring the potential difference between the ends of the annulus of known length and the mobility follows then as the ratio of the velocity and field intensity.

Relative mobility measurements are simpler. The mobility of a dye (brilliant blue) which does not change significantly over a wide pH range is determined once and for all. This dye is then injected along with the material under study[12]. The ratio of the distances of the two streaks from the zero-mobility reference streak at any point of the helical path is equal to the mobility ratio of the two materials under comparison. Since one of them is a substance of known mobility, a photograph of the separation pattern provides a measure of the unknown mobility.

7. CONCLUSION

Non-uniform magnetic fields exert forces upon particles submerged in a fluid of a magnetic susceptibility different from theirs. Establishing a gradient in magnetic susceptibility within the fluid in a non-homogeneous magnetic field offers the possibility of focusing particles in zones where the magnetic susceptibility of the fluid is equal to that of the particles (isomagnetic focusing). Thus, there exists the possibility of sorting particles in an "isomagnetic spectrum" in accordance with differences in their magnetic susceptibility values.

Inversion of the electromagnetic flowmeter effect results in electromagnetic pumping action. Such magnetohydrodynamic propulsion can be applied to an endless fluid loop maintaining it in constant circulation. This mechanism of fluid propulsion has the advantage that electromagnetic forces act upon each fluid element and that no pressure gradients have to be used to propell the fluid. As a result, a continuous-flow separation system can be achieved which does not require lateral membranes to create a closed channel for the flow of the buffer curtain. The omission of membranes eliminates drifts and spatial and temporal changes in pH and electrical conductivity

within the separation space of the fluid ribbon. In addition, the revolution of the buffer about a horizontal axis suppresses thermal convection and the particles to be separated which are orbiting in the circulating endless belt gain repeatedly constant increments in separation with each revolution. Thus, the particle path is wound up like a wire in a coil around an iron core and a long migration path can be accomodated in a compact apparatus.

Instead of generating fluid circulation, the combination of a current in an electrolyte with a perpendicular magnetic field can be used to generate a hydrostatic pressure gradient. Coupling of this hydrostatic force with a suitable gradient in electrical conductivity in the electrolyte column can be used to achieve stabilization against thermal convection similarly to density gradient stabilization. By superimposing such an electromagnetically activated conductivity gradient upon a density gradient, one can greatly augment the latter's effectiveness in stabilizing the fluid against thermal convection.

The combination of an electric current in a fluid with a perpendicular magnetic field makes it possible to generate in a closed body of fluid effects analogous to gravity and buoyancy. Particles differing from their surroundings in electric conductivity experience forces at right angles to the magnetic field and current. These forces vanish in an equiconductive environment and reverse their direction as the particle conductivity changes from a lower to a higher-than-environmental conductivity value. For biological cells the conductivity parameter is highly variable from one cell species to another, which makes this effect (electromagnetophoresis) of special interest for biological cell separations. In a gradient of electrical conductivity, electromagnetophoresis can sweep particles from all parts of a column toward zones where the electrical conductivity is equal to that of the particle. Such iso-conductivity focusing is analogous to isoelectric focusing and more closely so to isopyknic focusing in density. gradients. Among the aspects of electromagnetophoresis which may make it particularly attractive for biological cell separations are the possibilities (a) of using alternating currents (with alternating magnetic fields), (b) of conducting cell separations in biologically compatible media like blood serum, (c) of separating cells according to size and shape differences and finally (d) the feasibility of cell separations according to differences in two highly variable parameters: electrical conductivity and ionic cell membrane permeability. Electromagnetophoresis remained practically unused since 1954. There is a good likelihood that availability of superconducting magnets will stimulate its application to separations of cells and subcellular particles.

8. ACKNOWLEDGEMENTS

The earliest work received no grant support. Subsequently support was provided in sequence by The Office of Naval Research, Medical Testing Systems, Inc. and the American Cancer Society.

9. SUMMARY

The idea of the electromagnetic flow meter suggested experimental configurations which led to the ideas of electromagnetic pumping, electromagnetophoresis, electromagnetic stabilization against thermal convection, endless fluid belt electro-

phoresis, isoconductivity focussing, isoelectric focussing, isodielectric focussing, isomagnetic focussing, and, in general, isoperichoric focussing effects. Electromagnetophoresis is an effect which can be obtained in alternating or constant crossed electric and magnetic fields. Particles whose electrical conductivity differs from that of the surrounding fluid are set in motion irrespective of their electric charge (which may be zero). Separation effects are based on differences in the particles' electrical conductivities, size, shape and electrical membrane properties. In endless fluid belt electrophoresis electromagnetic pumping action maintains fluid circulation in an annular conduit in which axially electromigrating particles describe a helical path at the end of which they are intercepted and collected. Ideas of isoconductivity focussing, isoelectric focussing, isodielectric focussing, and isomagnetic focussing are byproducts of the aforementioned ideas.

REFERENCES

1 A. Kolin, An Electromagnetic Flow Meter—Principle of the Method and its Application to Blood Flow Measurements, *Proc. Soc. Exp. Biol. Med.*, 35 (1936) 53.
2 A. Kolin, Evolution of Electromagnetic Blood Flow Meters, *Pathophysiology of Congenital Heart Disease, U.C.L.A. Forum Med. Sci.*, 10 (1970) 383.
3 A. Kolin, An Electromagnetokinetic Phenomenon Involving Migration of Neutral Particles, *Science*, 117 (1953) 135.
4 A. Kolin, *Electromagnetophoresis*, in O. Glasser (Editor), *Medical Physics*, Vol. 3, Yearbook Publ. Co., Chicago, 1960, pp. 268–274.
5 D. Leenov and A. Kolin, Theory of Electromagnetophoresis, *J. Chem. Phys.*, 22 (1954) 683.
6 J. Kovalczik, *Electromagnetophoresis in Porous Media, Thesis*, Gdansk Polytechnic Institute, Gdansk, 1966, pp. 10–39.
7 J. C. Maxwell, *Treatise on Electricity and Magnetism*, par. 313, 3rd ed., Clarendon Press, Oxford, 1891.
8 A. Kolin, Centrifugal and Centripetal Electromagnetophoresis, *J. Appl. Physics*, 25 (1954) 1065.
9 K. K. Hannig, Eine Neuentwicklung der Trägerfreien Elektrophorese, *Hoppe-Seyler's Z. Physiol. Chem.*, 338 (1964) 211.
10 K. Hannig, Free Flow Electrophoresis, *Hoppe-Seyler's Z. Physiol. Chem.*, 356 (1975) 1209.
11 A. Kolin, Continuous Electrophoretic Fractionation Stabilized by Electromagnetic Rotation, *Proc. Nat. Acad. Sci. U.S.*, 46 (1960) 509.
12 A. Kolin and S. J. Luner, Continuous Electrophoresis in Endless Fluid Belts, *Anal. Biochem.*, 30 (1969) 111.
13 K. S. Cole and H. J. Curtis, in O. Glasser (Editor), *Medical Physics, Vol. I*, Yearbook Publ. Co., Chicago, 1944, pp. 344–348.
14 N. Catsimpoolas, S. Hjertén, A. Kolin and J. Porath, Unit Proposal: Tiselius Unit of Electrophoretic Mobility, *Nature (London)*, 259 (1976) 264.
15 W. P. Murphy, W. B. Dandliker and J. W. Keller, Magnetoelectrophoresis, *Transfusion*, 1 (1961) 367.
16 J. Kovalczik, *Electromagnetophoresis in Porous Media, Thesis*, Gdansk Polytechnic Institute, Gdansk, 1966, pp. 40–51.
17 A. Kolin, Method for Elimination of Thermal Convection, *J. Appl. Phys.*, 25 (1954) 1442.
18 A. Kolin, D. Leenov and W. Lichten, Electromagnetically Engendered Convection in Electromagnetophoresis, *Biochim. Biophys. Acta*, 32 (1959) 535.
19 A. Kolin, Separation and Condensation of Proteins in a pH Field Combined with an Electric Field, *J. Chem. Phys.*, 22 (1954) 1628.
20 A. Kolin, Isoelectric Spectra and Mobility Spectra: A New Approach to Electrophoretic Separation, *Proc. Nat. Acad. Sci. U.S.*, 41 (1955) 101.
21 A. Kolin, *Reminiscences about the Genesis of Isoelectric Focusing and Generalization of the Idea*, in B. J. Radola and D. Gräslin (Editors), *Electrofocusing and Isotachophoresis*, Walter De Gruyter, Berlin, New York, 1977, pp. 3–33.
22 A. Kolin, Electrophoretic "Line Spectra", *J. Chem. Phys.*, 23 (1955) 407.
23 H. Svenson and E. Valmet, *Sci. Tools*, 2 (1955) 11.

24 A. Kolin, Suppression of Thermal Convection and of Similar Types of Fluid Streaming by an Electromagnetic Force Field, *Biochim. Biophys. Acta*, 32 (1959) 538.
25 A. Kolin, Kinematic Stabilization of Continuous-flow Electrophoresis Against Thermal Convection, *Proc. Nat. Acad. Sci., U.S.* 51 (1964) 1110.
26 S. Hjertén, Free Zone Electrophoresis, *Ark. Kemi*, 13 (1958) 151.
27 A. Kolin, Preparative Electrophoresis in Liquid Columns Stabilized by Electromagnetic Rotation. Part 1: The Apparatus, *J. Chromatogr.*, 26 (1967) 164.
28 A. Kolin, Preparative Electrophoresis in Liquid Columns Stabilized by Electromagnetic Rotation. Part II: Artifacts, Stability and Resolution, *J. Chromatogr.*, 26 (1967) 180.
29 B. Bergrahm, Apparatus for Zone Electrophoresis in Vertical Column, *Science Tools*, 14 (1967) 34.
30 S. J. Luner, *Electrophoretic Studies of Isolated Mammalian Metaphase Chromosomes, Thesis*, Univ. of California, Los Angeles, Calif., 1969.
31 A. Kolin, *Cell Separation by Endless Fluid Belt Electrophoresis*, in N. Catsimpoolas (Editor), *Methods of Cell Separation*, Vol. 2, Plenum Publ. Co., New York, 1978, in press.
32 A. Strickler and T. Sacks, in N. Catsimpoolas (Editor), *Isoelectric Focusing and Isotachophoresis*, N.Y. Acad. Sci., New York, 1973, pp. 497–514.
33 A. Kolin and S. J. Luner, in S. G. Perry and C. J. Van Oss (Editors), *Progress in Separation and Purification*, Wiley, New York, 1971, pp. 93–132.
34 A. Kolin, *Endless Belt Continuous Flow Deviation Electrophoresis*, in P. G. Righetti, C. J. Van Oss and VanderHof (Editors), *Electrokinetic Separation Methods*, Elsevier/North-Holland, Amsterdam, 1978, in press.
35 A. Kolin and B. Ellerbroek, Thermal Convection in a Vertical Fluid Sheet, to be published.